Master Thesis

Institute of Applied Geosciences
Graz University of Technology

Institute of Earth Sciences
University of Graz

The Influence of Extensive Slope Tectonics on the Hydrogeological System Roach Spring (Carinthia/Austria)

Author

Raphael Staunig

Advisors

VAss. Mag. Dr. Gerfried Winkler
Univ.-Prof. Mag. Dr. Walter Kurz

STATUTORY DECLARATION

I herewith declare that I have completed the present thesis independently making use only of the specified literature and aids. Sentences or parts of sentences quoted literally are marked as quotations.

…… date

…….. (signature)

Acknowledgements

For their support and patience throughout the work on this thesis, I would like to thank:

my advisors Gerfried Winkler and Walter Kurz,
Peter Reichl and Walter Poltnig from Joanneum Research,
Mr. Kleewein and Mr. Standman from the building yard of the city Velden am Woerthersee,
Federal State Government of Carinthia, especially for their financial support,
Ashley Sweet,
and my family.

Index

Abbreviations and Definitions 6
Abstract 7
Kurzfassung 8

1 Introduction
1.1 Idea 9
1.2 Geographic Overview 12

2 Basics
2.1 Geologic Overview 12
2.1.1 Klagenfurt Basin 14
2.1.2 Regional Structures 15
2.1.3 Detailed Geological Overview of Turiawald 16
2.1.4 Mass Movements and Geomorphology 19
2.2 Hydrogeologic Overview 21
2.3. Theory of Mass Movements and Deformation 23
2.3.1 Formation and Classification 23
2.3.2 The System “Hard on Soft” 25
2.4 Structural Geology and Tectonics 26

3 Methods
3.1 Field Mapping 27
3.2 Structural Analysis 28
3.3 Analysis of Lineaments and Topography 28
3.4 Hydrogeologic Monitoring 29
3.5 Theory of Discharge Analysis 30
3.5.1 Hydrograph 30
3.5.2 Quotient of Discharge 30
3.5.3 Coefficient of Discharge 31
3.5.4 Natural Tracers 33

4 Results
4.1 Structural Geology 34
4.1.1 Outcrop St.Ruperti 34
4.1.2 Outcrop Oberdoerfl 36
4.1.3 Turiawald Rock Faces 36
4.2 Geomorphology 39
4.2.1 Regional Lineaments 39
4.2.2 Turiawald Plateau 41
4.2.3 Turiawald Western Slope 44
4.3 Hydrogeology
4.3.1 Hydrogeologic Mapping 48
4.3.2 Aquiclude of Western Turiawald 48
4.3.3 Hydrogeologic Monitoring 50
4.3.4 Resources of Water 56

5. Discussion Interpretation
5.1 Structural Geology and Geomorphology 59
5.1.1 Turiawald Plateau 59
5.1.2 Mass Movement of the Western Slope 60
5.2 Hydrogeology 62
5.2.1 Aquiclude Morphology 62
5.2.2 Hydrograph Analysis and Natural Tracers 63

6. Conclusion
6.1. Failure Mechanism and Kinematics 66
6.2 Hydrogeology 68

7.Literature 69

Appendix A 74

1. Ombrograph data 74

2. Structural data 74

Appendix B 80

Abbreviations and Definitions

centimetre = cm
electric conductivity = ec
digital elevation model = dem
discharge = litres per second = (l/s)
figure = fig.
joint openings = open discontinuities with an aperture of more than one metre
litres = (l)
metre = m
metres above sea level = m.a.s.l.
micro Siemens per centimetre = µs/cm
millimetre = mm
million = mill.
square kilometre = km^2
table = tab.
temperature °Celsius = T℃

Abstract

The westernmost part of the Sattnitz Mountains (Carinthia, Austria) is the detached plateau Turiawald, which has an elevation of 880 m and a surface area of 6 km². Its hanging wall consists of the Sattnitz Conglomerate and the footwall is comprised of the Penken Formation which are fine clastic sediments in the NW and uplifted crystalline basement in the SE. The plateau is characterized by widespread break up of the conglomerate layer, and is classified as a “hard on soft” system of failure. The western slope of Turiawald is affected by a large, complex mass movement.

The hanging wall layers act as an aquiclude, the conglomerate as an aquifer. There is no surface runoff from the plateau, since all infiltrating precipitation is discharged from Roach Spring in the northwest and several strongly discharging springs in the north. Roach Spring, which drains ~75-80% of the Turiawald Plateau, is situated at the base of the large area mass movement. The springs in the north flow directly from the plateau conglomerate layer. Based upon multiannual discharge data obtained from the Roach and Pleier Springs, as well as natural tracers such as electric conductivity and temperature, the characteristics of discharge and groundwater storage were analysed, to determine the influence of the mass movement on the Roach Spring. The two coefficients of discharge (α-values) for Roach Spring, have a magnitude of 10 E-1 (event water) and 10 E-2 (base flow) as well as a quotient of discharge of ca. 0.05. Roach Spring has a hydraulic reaction within one day of a precipitation and a time lag of ~four days until minimum electric conductivity is reached. The three coefficients of discharge of Pleier Spring have a magnitude of ~10 E-2 (2 x event water) und 10 E-3 (base flow) and a quotient of discharge of ~0.3. Pleier Spring shows a hydraulic reaction within one to three days of a precipitation and a time lag of ca. 15 hours until minimum electric conductivity is reached. Unlike Roach Spring, the electric conductivity of Pleier Spring rises again to its original level after a short time. The catchment area of Pleier Spring (plateau area) features a small storage of relatively fast permeability (fracture system of the plateau), as well as a large, less permeable storage (narrow joint/matrix system). The catchment area of Roach Spring consists of two parts: an extremely permeable and quickly discharging storage (void system of the mass movement debris) and the mixture of this mass movement storage and the large but less permeable storage (joint system of the western plateau).

Kurzfassung

Der westlichste Teil der Sattnitzberge (Kärnten, Österreich) ist der Turiawald, ein abgesetztes ca. 880 m hohes, über 6 km² großes Plateau. Im Hangenden steht das Sattnitzkonglomerat (Pontium) an, welches im Norden und NW von feinklastischen Sedimenten der Penken Formation (Pliozän/Pleistozän) und im Südosten von aufsteigendem permotriassischem kristallinem Basement unterlagert wird. Das Plateau ist durch ein großflächiges Zerbrechen der Konglomeratschichten, was als „hart auf weich" System klassifiziert wurde, gekennzeichnet. Zudem weist der Westhang des Turiawaldes eine komplexe großflächige Massenbewegung auf.

Die Liegendschichten wirken als Grundwasserstauer, das Konglomerat als Grundwasserleiter. Es existiert kein Oberflächenabfluss, sodass der gesamte infiltrierende Niederschlag an der Roachquelle im Nordwesten und mehreren, großen Quellen im Norden austritt. Die Roachquelle, welche ca. 75-80% des Turiawaldplateaus entwässert, liegt am Fuße der großflächigen Massenbewegung, die Quellen im Norden (z.B. Pleierquelle) treten direkt aus den Konglomeratschichten des Plateaus aus. Basierend auf mehrjährigen Schüttungsdaten der Roach- und der Pleierquelle sowie anhand der natürlichen Tracer, elektrische Leitfähigkeit und Wassertemperatur, wurde das Auslauf- und das Speicherverhalten untersucht, um den Einfluss der Massenbewegung auf die Roachquelle zu erfassen. Die Roachquelle weist zwei Auslaufkoeffizienten (α-Werte) von ca. 10 E-1 (Eventwasser) und 10-2 (Basisabfluss) und einen Schüttungsquotient von ca. 0.05 auf. Sie zeigt eine hydraulische Reaktion auf ein Niederschlagsereignis innerhalb eines Tages und Time-lags der Leitfähigkeitsminima von ca. vier Tagen. Die drei Auslaufkoeffizienten der Pleierquelle liegen bei ca. 10 E-2 (Eventwasser), und 10 E-3 (2 x Basisabfluss), ihr Schüttungsquotient bei ca. 0.3. Sie zeigt eine hydraulische Reaktion auf ein Niederschlagsereignis nach ca. ein bis drei Tage und Time-lags der Leitfähigkeitsminima von ca. 15 Stunden. Im Gegensatz zur Roachquelle wird die Ausgangsleitfähigkeit wieder rasch erreicht. Das Einzugsgebiet der Pleierquelle (Plateaubereich) ist durch einen gut durchlässigen, geringen Speicher (Bruchhohlraumsystem des Plateaus) sowie durch einen gering durchlässigen, großen Speicher (Feinkluft-/Matrixsystem) gekennzeichnet. Das Einzugsgebiet der Roachquelle wird dagegen durch einen deutlich höher durchlässigen Speicher gekennzeichnet (Hohlraumsystem der Massenbewegung), welcher ein rasches Auslaufen bewirkt. Dieser überprägt einen weiteren, geringer durchlässigen großen Speicher (Kluftsystem des Westplateaus).

1 Introduction

1.1 Idea

The plateau mountain Turiawald is affected by break up phenomena, in addition a large scale mass movement is situated on its western slope. Several springs drain this geologic system, showing highly different discharge rates. The strongest discharging spring is situated at the base of the mass movement, while the other springs show much lower discharge rates. This situation brought up the question, in what way is the discharge behaviour influenced by the mass movement?

To describe the hydrogeologic conditions which cause the different discharge rates, two springs, one influenced by the mass movement and one not, were compared by analysis of spring logging data.
This was done by characterisation of the two investigated springs in hydrogeologic ways. Differentiation of base flow and event water as well as an estimation of the theoretical available resources of water were calculated from the collected data. To get a representative data base for this purpose, both springs were monitored by data loggers over a period of four years.

Other information relevant to the influence of the mass movement on the spring discharge is the spread and type of the mass movement and the mode of failure, for both the in situ rock mass and the mass movement body. Furthermore, the position of the aquiclude on the western slope of the working area was determined.
Probably linked to failure kinematics of the mass movement and the structure of the plateau are also regional geological factors, which affect the basement and top layers of the investigated area. The structural situation of these formations was described and interpreted.

1.2 Geographic Overview

The Sattnitz Mountains are located north of the Karawanken Mountains on the southern rim of the Klagenfurt basin in Carinthia, Austria. The 30 km long, 7 km wide and up to 900 metre high plateau-like ridge is west-east oriented. It features several rock faces up to 100 metre high and is divided by the north-south striking Koettmannsdorfer depression into eastern Sattnitz and western Sattnitz. The westernmost part of the western Sattnitz is the Turiawald (Turia Forest), which is a plateau situated close to the villages Roach and Penken (fig.1), and is the focus of this study. The investigated area and its western foreland are completely covered by woodland**.**

(fig.1): The upper figure shows map of the Sattnitz Mountains in Carinthia. The blue rectangle marks the study area Turiawald; scale 1:175000. The lower figure shows an enhanced view of the blue rectangle, scale 1:23000 (BEV, 2010)

The Sattnitz Mountains are affected by several mass movements and slope instabilities, ranging in scale from minor scarps and tilted blocks to mountain splitting phenomena. Furthermore, this ridge functions as catchment area for several springs which supply drinking water to the adjacent communities.

.

2 Basics

2.1 Geologic Overview

In the southeastern Alps the Periadriatic Line, a fault system crossing the Alps from the Thyrrenian Sea to the Pannonian basin, separates the Southalpine unit from the northern Central Austroalpine unit (fig.2) (Laubscher 1970, 1983, 1988, Bögel 1975, Schmid et al. 1989, von Gosen 1989).

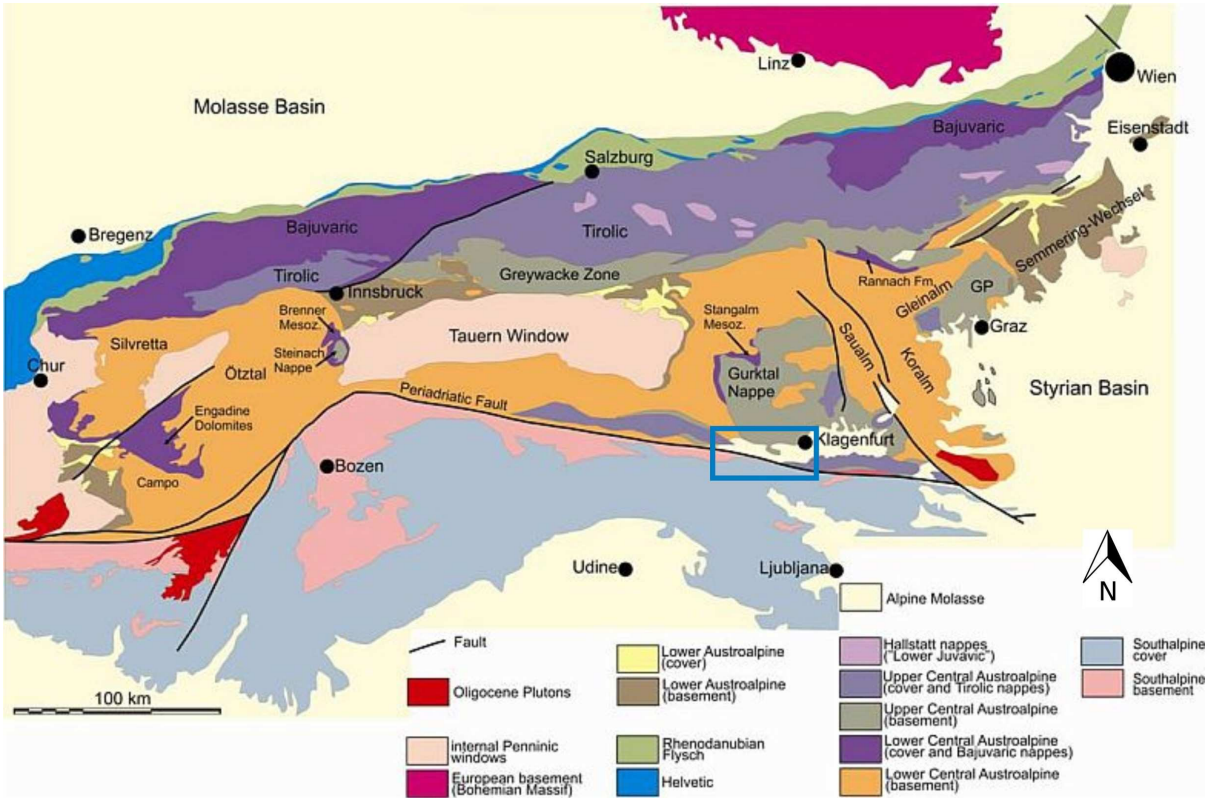

(fig.2): Geologic map of the Eastern Alps. The blue rectangle marks the study area (modified after Kurz 2010, unpublished map with courtesy of Kurz)

Both the Central Austroalpine and Southalpine units comprise Permo-Mesozoic platform strata as cover, which rest on a metamorphosed Paleozoic Variscan basement (Brandner 1972, Bögel 1975, Niedermayr 1975, Tollmann 1977, Laubscher 1988).

Along the Periadriatic Line, the Austroalpine basement, which is part of the Gurktal Nappe system, includes Ordovician metavolcanoclastics, micaschists, phyllites, marbles and Permian granite, which is overlain by Permian redbeds. The Central Austroalpine cover is a 3.4 km thick Upper Permian to Lower Cretaceous sequence, mainly consisting of dolomite and limestone units of the Triassic Wetterstein and Hauptdolomit formations, which are overlain by basinal Jurassic to Cretaceous limestones and marls (Schönlaub 1979, Bauer et

al. 1983). The Neogene syntectonic clastics of the Klagenfurt Basin overly the Austroalpine strata (Polinski et al.1992). The Southalpine unit is 3.2 km thick and consists of Ordivician to Lower Carboniferous metasediments as basement, overlain by Upper Carboniferous to Jurassic sedimentary strata, mainly marine clastics and carbonates (Schönlaub 1979, Bauer et al. 1983) (fig.3).

The Karawanken Mountains consist of both Austroalpine and Southalpine units and straddle the Periadriatic fault. Miocene dextral strike slip deformation along this fault zone and thrust displacement along the northern Karawanken front initiated the subsidence of the Klagenfurt Basin (Polinski et al.1992).

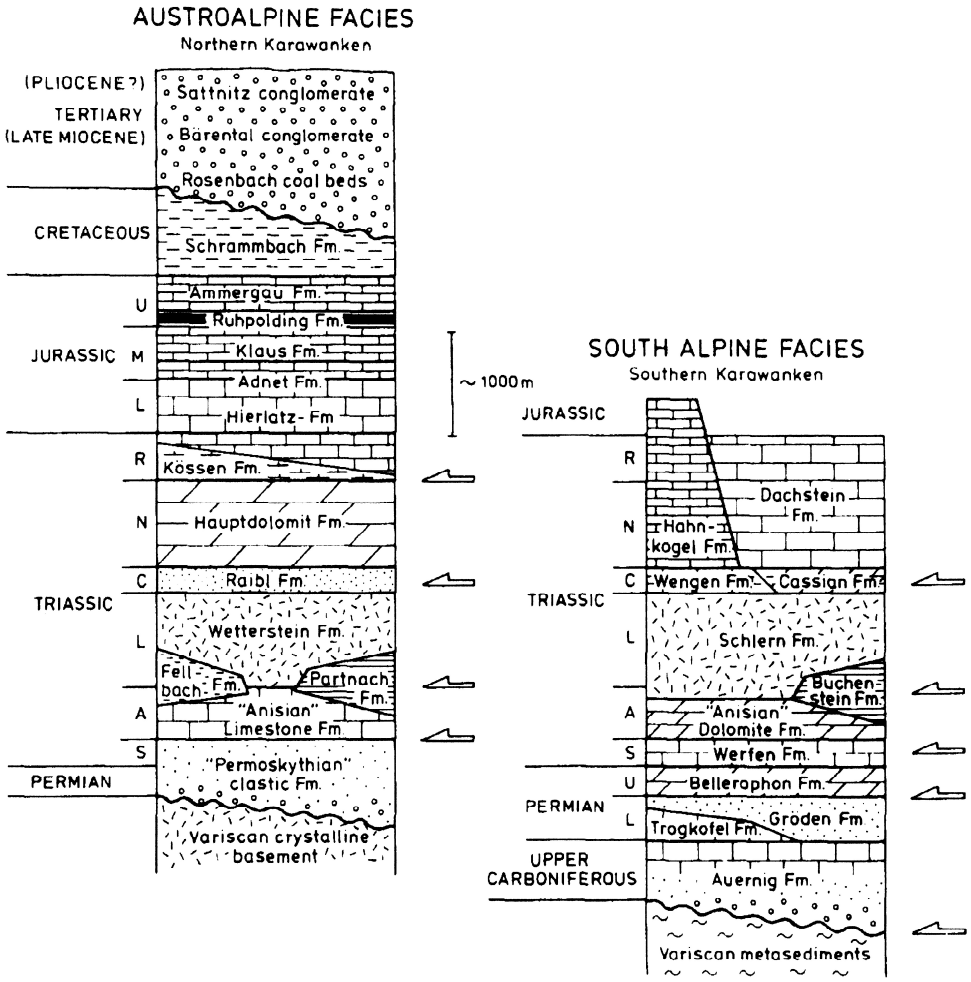

(fig.3): Stratigraphic units of the Austroalpine and Southalpine facies domains juxtaposed along the Periadriatic Line and showing the distinct mismatch of sedimentary facies. Triassic stages are abbreviated with letters. Potential detachment horizons within the Mesozoic cover sequence are indicated by open arrows (Polinski et al.1992).

2.1.1 Klagenfurt Basin

The Klagenfurt Basin is an east-west orientated intra orogenic basin of Sarmatian to Quarternary age (fig.4) (Nemes et al.1997). During the late Miocene, upwards northwest directed nappe stacking and flexure of the Austroalpine lithosphere was initiated by loading through the Karawanken unit during its approach from the south, kinematically connected to brittle transpressive strike slip deformation along the Periadriadic Fault (Nemes et al.1997). The final northwest directed overthrust of the Karawanken unit over the Neogene Sediments of its foreland took place in Pliocene times. Linked to brittle transpressive shearing along the Periadriatic fault, the basin and a positive flower structure were formed, and the foreland was flexured again (fig.5, Nemes et al.1997).

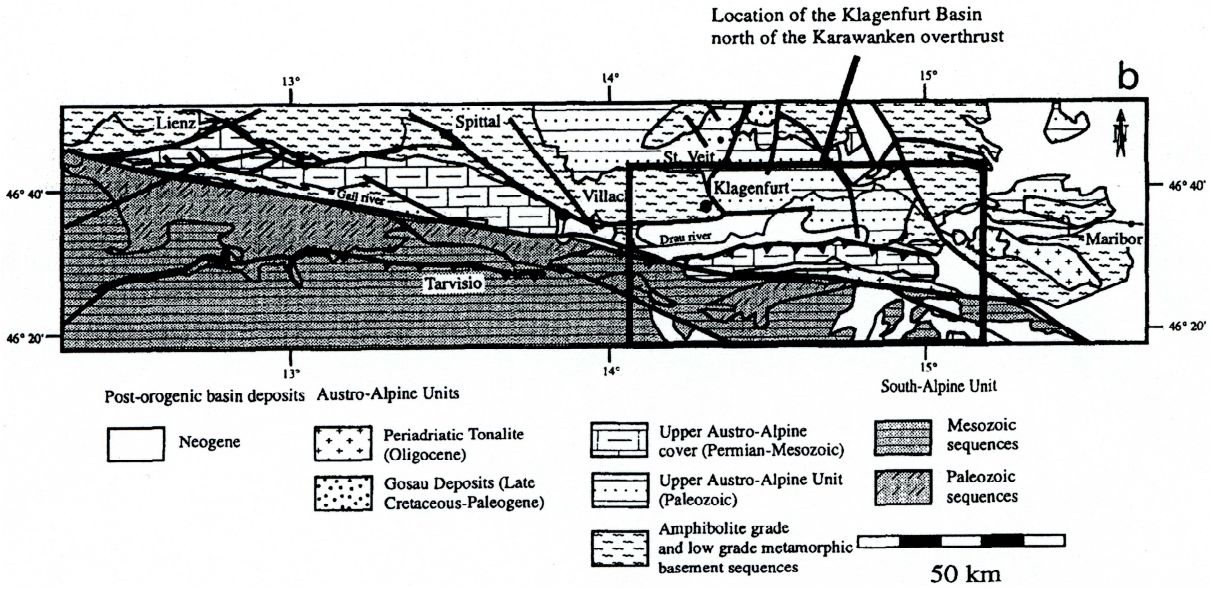

(fig.4): Location of the Klagenfurt Basin (Nemes et al.1997)

The stratigraphy of the Klagenfurt Basin comprises a more than 1000 m thick Sarmatian to Quarterny sequence, deposited on Austroalpine basement units, which starts with the Rosenbach Formation (early Sarmatium), containing limnic, coal bearing, fine grained sediments (Kahler 1953). The formation is divided into a lower, coal bearing part and a coarsening upward sequence. Lower coal bearing sections include mudstones, sandstones and coarse conglomerates with interbedded carbonate, while the upper sequence of the Rosenbach Formation comprises an over 100 m thick coarse conglomerate bearing layer derived from the uprising Karawanken Mountains and rocks from the Austroalpine metamorphic basement with some mud- and sand bearing clastics interbedded (Papp 1951, Klaus 1956; Tollmann 1985). These are again overlain by thick, coarse, carbonate bearing conglomerates. The Baerental Conglomerate overlies the latter with a thickness of several

100 m (Pannonium - Pontium). Northward it grades into the Penken Formation, a coal bearing up to 50m thick siltstone layer (Pontium) (Kahler 1953). The uppermost most part of the stratigraphic sequence is the up to 200m thick Sattnitz Conglomerate (Pliocene - Pleistocene) (Tollmann 1985).

2.1.2 Regional Structures

The Periadriatic Fault and its related structures are a first order boundary between the Austroalpine and Southalpine units. During Miocene times, northwest directed nappe stacking north of the Periadriatic Fault was followed by overthrusting of the Karawanken massive which formed a positive flower structure, associated with flexure of the foreland and formation of the Klagenfurt basin (Nemes et al.1997). Final NNW directed overthrust of the Karawanken Mountains onto the foreland is characterized by NW–SE striking dextral tear faults and NW to NNW directed thrust planes in the Neogene Sediments of the Klagenfurt basin (fig.6). NNW-SSE directed contraction formed transpressional structures depicted by NNW-directed thrusts and SSE-directed backthrusts, NW-striking dextral faults (R faults), and NE-striking sinistral faults (R' faults) (Nemes et al.1997). To the south, both Rosenbach Formation and the overlying Bärental Conglomerate are overthrusted by the North Karawanken unit and folded, indicating a reverse anticline, while S-dipping thrusts and reverse faults override the Sattnitz Conglomerate (Kahler 1953).

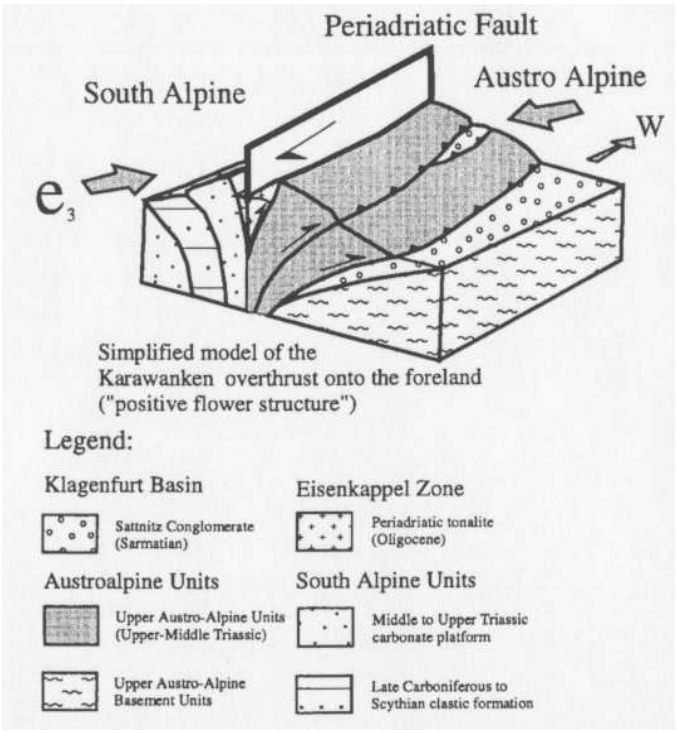

(fig.5): Sketch showing the Karawanken overthrust onto the foreland ("positive flower structure") (Nemes et al.1997)

2.1.3 Detailed Geological Overview of Turiawald

The NW/SE striking Hochstuhl fault (fig.6) intersects the Periadriatic Fault and divides the paleozoic basement and permotriassic cover units west of Turiawald in western and eastern parts. To the west, a greenschist metamorphic phyllite basement is overlain by permotriassic clastic conglomerates, quarzites, sandstones (Werfener Schichten) and triassic carbonates (Anisium) (Claasen et al. 1987). East of the fault, diaphtorites, micaschists, marbles, phyllites, isolated amphibolites and greenschists build up prepermian basement units, which are overthrusted by dolomites of Anisian and Ladinian age, as well as Triassic calcitic marble (Claasen et al. 1987). Mylonitisation occurs in both basement and cover rocks along their shear planes, especially dolomites show fault breccias and cataclasites. Younger Triassic to Jurassic units were probably sedimented, but have been eroded in upper Cretaceous times (Claasen et al. 1987). Lithologies are displayed in figure 7.

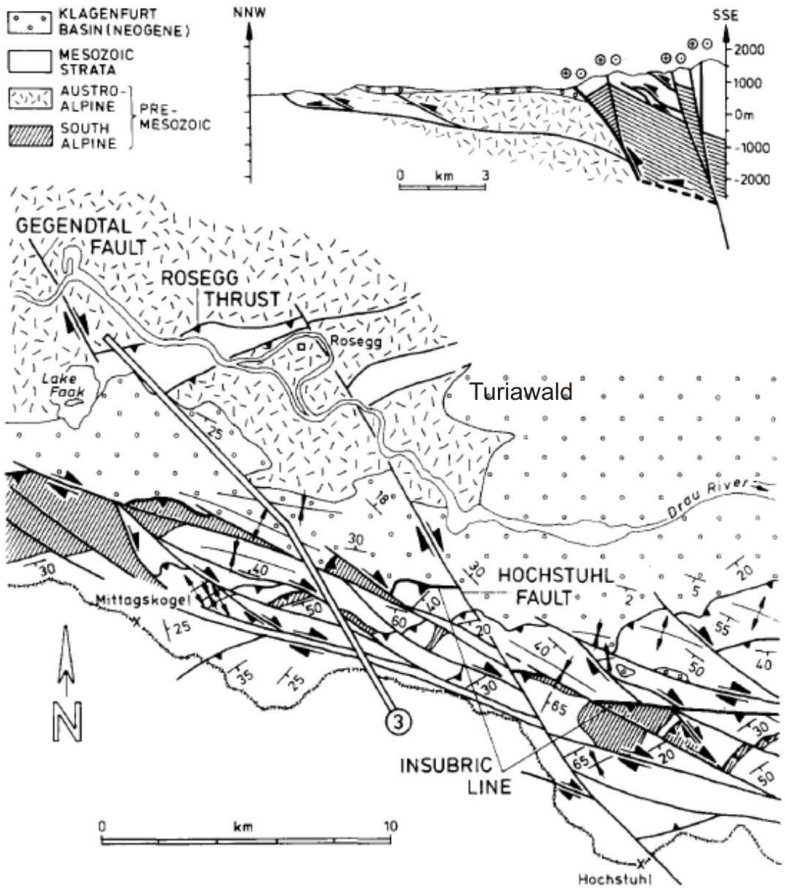

(fig.6): Sketch map and cross section of the Hochstuhl Fault and the Periadriatic Line SW of Turiawald (modified after Polinski et al.1992)

Two prealpine and three alpine deformations affected both paleozoic and permotriassic rocks. While prealpine deformations are not preserved, the alpine deformations can be

distinguished (Claasen et al. 1987). The first alpine deformation led to folding with NNW/SSE to NNE/SSW striking b-axes which dip to the south in phyllites and marbles, where also joints parallel to b-axes opened. The second alpine deformation created N vergent W/E striking folds which dip to the west. Additionally, in permotriassic carbonatic and clastic rocks, particularly in dolomites, N/S striking vertical joints as well as two conjugated sets of oblique fractures were opened. During the second deformation, fault breccias and cataclasites were also formed in dolomites (Claasen et al. 1987). The third alpine deformation is poorly preserved.

Miocene brittle tectonics formed nearly vertical NNE/SSW to NNW/SSE striking faults, which affect both paleozoic and permotriassic rocks. Their striking is also parallel to joints formed during the first alpine deformation. NW/SE striking faults can be found in marbles west of Turiawald (Hochstuhl fault, fig.6), and Triassic dolomites of Kathreinkogel show NW/SE joints that are not related to alpine deformation. Further west, a nearly vertical, south dipping, W/E orientated normal fault exists (Claasen et al. 1987).

Two lithostratigraphic units of neogene age can be differentiated at the Turiawald Plateau (fig. 7 and 8):

The footwall comprises the basal fine clastic rocks of the Penken Formation, 30 to 70 m thick limnic sediments with coal deposits interbedded in the upper parts of the strata (Pontium).
The hanging wall is the Sattnitz Conglomerate, 150 to 200 m thick and in general dipping flat towards the south with some sandstone layers in between (Pliocene-Pleistocene) (Griem et al.1992). It contains coarse clastic gravel and is divided into two conglomerate types: Type Tanzboden has more than 74% carbonatic gravel and less than 10% crystalline gravel, type Turia has less than 60% carbonatic gravel and more than 18% crystalline gravel (Griem et al.1992). Lithologies are displayed in figure 7. The majority of the components embedded in a carbonatic matrix were deposited during the uprising of the Karawanken Mountains. The crystalline components originate from western and northwestern regions of the Central Austroalpine unit, the Drauzug and the Tauern Window (Griem et al.1992).

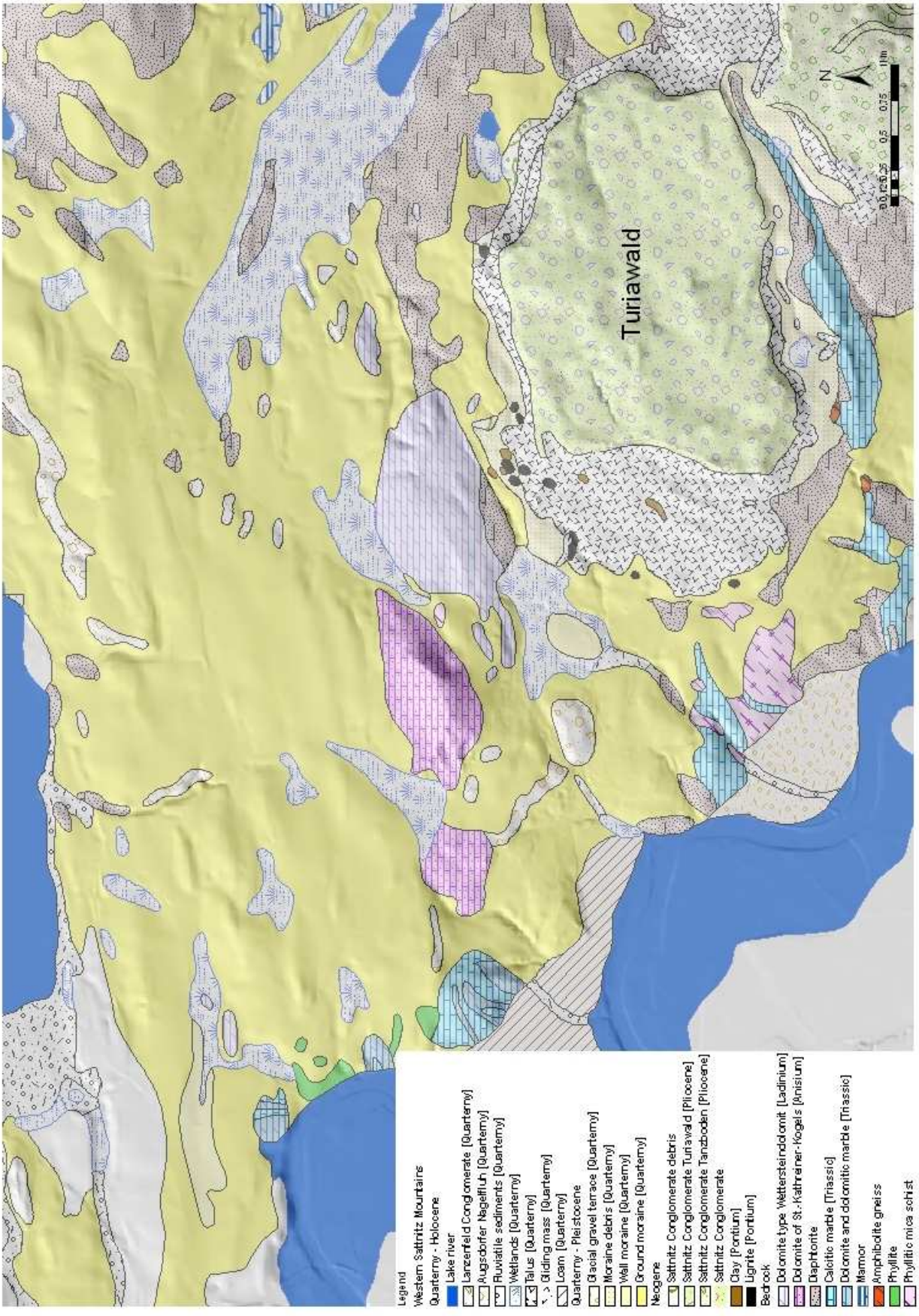

(fig.7): Lithological map of the Turiawald Plateau and its western foreland (modified after Poltnig et al. 2007)

The thickness of the basal fine clastic rocks of the Penken Formation decreases from NW to SE (fig.8). A sedimentary, discordant contact between metamorphic basement units, i.e. marbles and diaphtorites, and the coarse clastics of the Sattnitz Conglomerate is exposed south of Turiawald (Griem et al.1992). Coals interbedded in basal fine clastic rocks were explored until the 1950´s. Surface and subsurface mining was done on the western and northwestern slopes of the Turiawald Plateau.

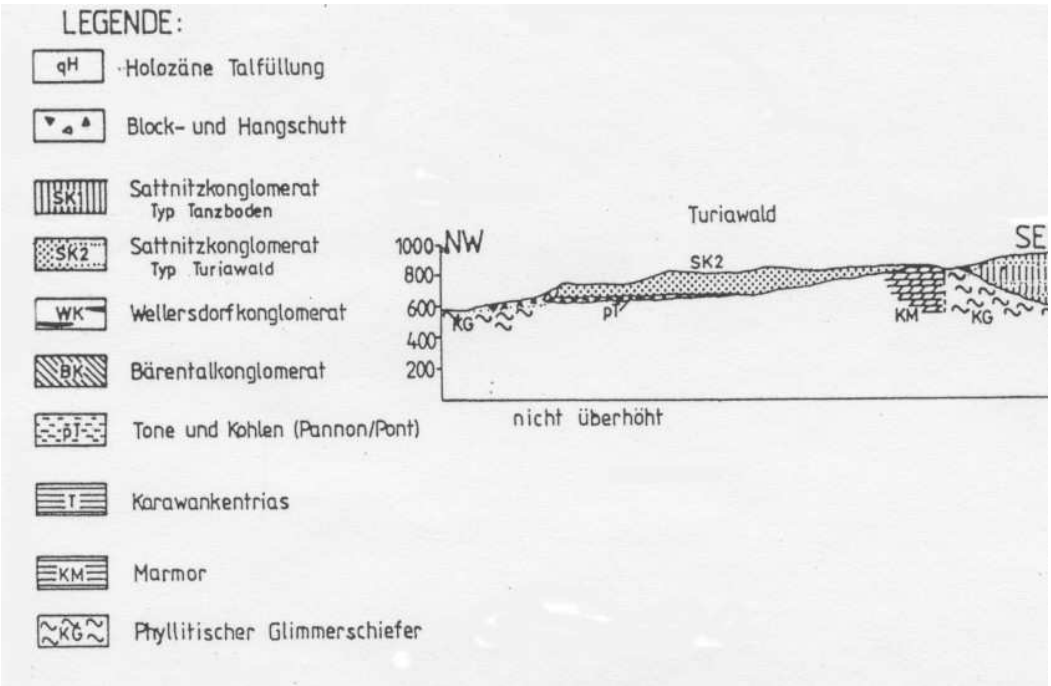

(fig.8.): Sketch of the cross section of the Turiawald Plateau (Griem et al.1992)

2.1.4 Mass Movements and Geomorphology

The Sattnitz Conglomerate is divided into four separate parts by large scale lineaments. Turiawald is separated from the Tanzboden Plateau in the southeast by faulting. Large scale lineaments striking N/S and NNW/SSE divide Tanzboden from the western Koettmannsdorf area and a NW/SE striking lineament separates the latter from eastern Koettmannsdorf area (Winkler et al. 2008).

The western Sattnitz Mountains are affected by several small and large scale mass movements. Downward moving conglomerate blocks appear along the entire border of the Plateau. Located north of the western Sattnitz Mountains is the large scale mass movement of Dobein, with an extent of about 4.5 square kilometres (Fellner 1993). Moraine sediments found in this area indicate glacial overprint (Poltnig et al. 2007).

The Tanzboden Plateau southeast of Turiawald shows slope tectonic phenomena. Its western slope features tower shaped conglomerate blocks moving downwards. On the

plateau itself, sinkholes and depressions can be found and it is divided by a WNW/ESE striking fault line (Fellner 1993).

Turiawald is separated from the main conglomerate plateau and bordered by steep rock faces. Its surface shows large numbers of sinkholes and depressions. Both karstification and tectonic movements are assumed as the cause for formation of the sinkholes (Fellner 1993, Poltnig et al. 2007). The western slope of the Turiawald is characterized by a large area mass movement. Series of downward moving blocks have formed an undulous morphology, depicted by wall and trench structures. At the north western break off, a large conglomerate block (about 200 m in diameter) is deposed from the plateau and lowered several tens of metres (Fellner 1993, Winkler et al. 2008).

The morphology of Turiawald and its western foreland is affected by glacial overprint. During pleistocene times, the overall area was covered by glacial ice. Moraine material can be found in tectonically induced depressions, especially in the southern parts of the Sattnitz Mountains (Winkler et al 2006). During the Wuerm glaciation, the Sattnitz Conglomerate was overthrusted several hundreds of metres by the Drau Glacier, which was flowing from W to E. The glacial overprint of Sattnitz Conglomerate is assumed to be a major factor in the formation of the mass movements, since the ice acted as a counter bearing for the western slopes (Fellner 1993).
Transport of the coarse clastic sediments to the deposition area was made possible by a braided river system, running from W to E, transgressing over afore deposited clastics and coals as well as exposed paleozoic basement (Griem et al.1992).

2.2 Hydrogeologic Overview

The N and NW parts of the Sattnitz Conglomerate of Turiawald are underlain by neogene fine clastic rocks of the Penken Formation (fig.8), the S and SE parts by prepermian marbles and diaphtorites (Griem et al.1991, Poltnig et al. 2007). The conglomerate and its debris act as an aquifer, the subjacent clastic and crystalline rocks as an aquiclude (Poltnig et al. 2007). All springs seem to be more or less located at the contact between aquifer and aquiclude (fig.9). The aquiclude run is not verified on the western slope, due to the influence of the mass movement in this area. It is assumed that the aquiclude is displaced and deformed by slope tectonics (Winkler et al 2008, Poltnig et al. 2007).

The Pleier Spring at the northern flank of Turiawald lies at about 650 m above sea level (fig.9). The water gallery Hojoutz is located ca. one kilometre south east of Pleier at an elevation of 645 metres (fig.9). At the eastern slope at an altitude between 640 and 700 metres, two springs are situated (fig.9) where the conglomerate is in contact with the basal fine clastic rocks. At the southern slope above the village of St.Ruperti, two other springs at an altitude of 760 and 780 metres are found (fig.9) and show little discharge compared to the other springs. The Roach Spring is situated on the western slope at the base of the mass movement at ca. 550 m above sea level (fig.9), a remarkably lower altitude than the anticipated position of the neogene coal bearing fine clastic rocks in this area (Poltnig et al. 2007).
Roach Spring has the strongest discharge of all springs of Turiawald (ca. 75 % of the total discharge, Poltnig et al. 2007) and is used as a drinking water supply. Pleier and Hojoutz Springs are also being used as sources of drinking water and show relatively higher discharge compared to the southern and eastern springs of Turiawald (Poltnig et al. 2007).

The plateau is underlain by impermeable rocks and shows no surface water runoff. Therefore, the whole infiltrating precipitation (excluding evaporation) is drained by spring discharge. Spring discharge from surface runoff and springs of adjacent areas show when compared that discharge from Turiawald is evenly balanced, which also indicates that all infiltrating precipitation is drained by the known springs at the plateau escarpents (Poltnig et al. 2007).

The hydrologic recharge area of Turiawald (6.1 km², fig.9) shows an average discharge of 106.1 (l/s) for the years 2005 to 2006 . Roach Spring has a recharge area of 3.9 km² and discharges 88.3 (l/s) in average, Pleier Spring has 0.8 km² recharge area and an average outflow of 17.8 (l/s) (including Hojoutz water gallery discharge). Discharge volumes of the

single springs described above are listed in figure 9. The groundwater measured at the springs is well stored and has an age of approximately five years (Poltnig et al. 2007).

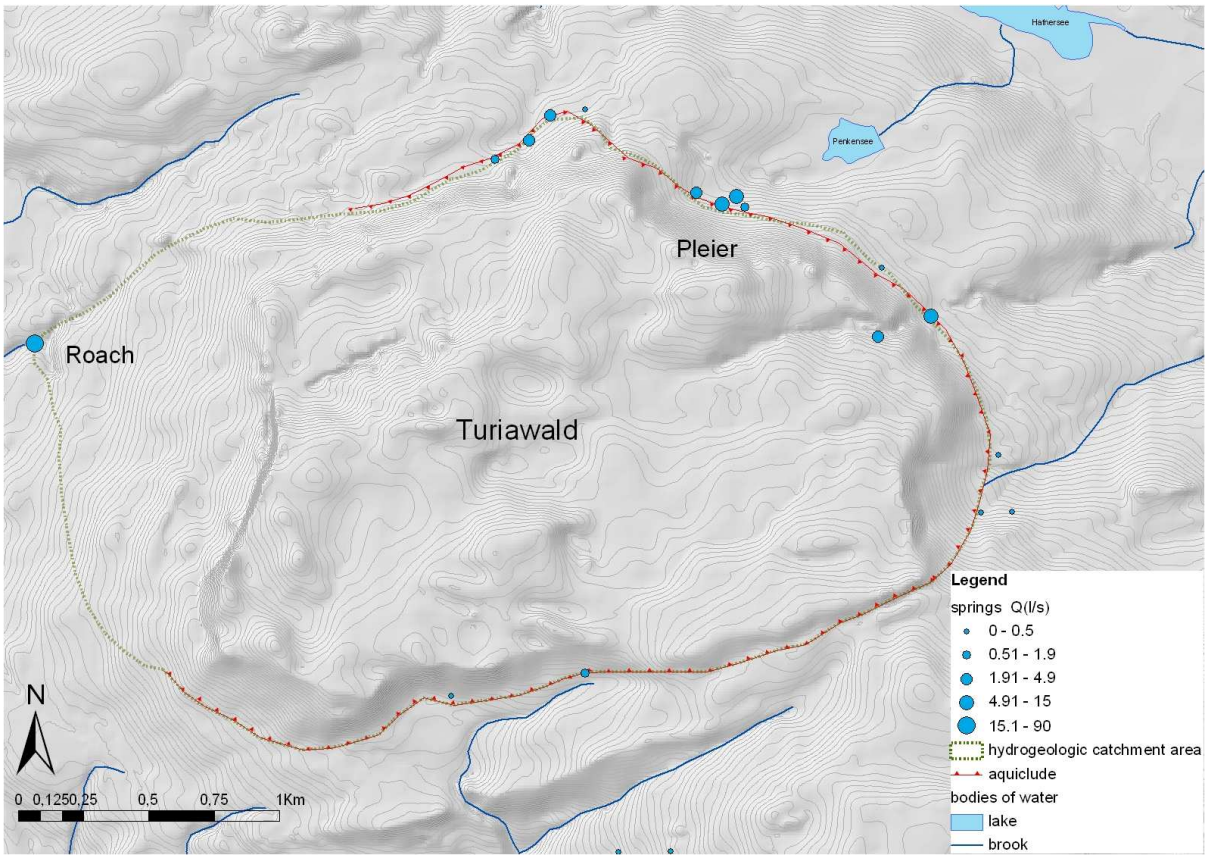

(fig.9): Turiawald Plateau, hydrogeologic catchment area and verified aquiclude run. The size of the blue dots marking springs is relative to the discharge volume from the years 2005 to 2006 (modified after Poltnig et al. 2007)

2.3. Theory of Mass Movements and Deformation

2.3.1 Formation and Classification

Valleys and dells are formed when glaciers and rivers cut themselves into the ground surface. Normally these newly developed depressions have over steepened slopes. Due to erosion, weathering, and gravitational forces, over steepened slopes start to flatten out through the downward movement of material.
A mass movement is a valleyward directed transport of soil or rock mass which takes place if destabilizing forces such as gravitation, water pore pressure, or triggers like rapid increase of stress (earth quakes or volcanoes) overcome retaining forces such as strength of slope material and friction. If a mass movement has a variety of causes and fails gradually, a trigger is not strictly necessary (Whyllie, Mah 2004).

The kind of deformation is dependent on the type and geological structure of the rock mass or soil. Within a mass movement, several different mechanisms of deformation and movement can take place at the same time due to jointed and fractured rock, weak materials, or differences in water permeability or stiffness. Large area gravitational slope deformations of an entire mountainside can occur at slopes that have been over steepened by glacial or fluviatile erosion. If the glacier retreats, the ice no longer acts as a retaining and supporting factor due to its weight and the slope starts to move until an equilibrium of forces is achieved again (Hutchinson 1988, Madritsch, Millen 2007).

There are different classifications for mass movements and landslides. Based on mechanic behaviour and speed of movement, the following types can be distinguished:
Creep and viscous flow are constant movements over time; a single plane of failure cannot be determined. Sliding is a movement of rock mass along one ore more sliding planes. Mudflow, earth flow and debris flow are types of movement in rock mass or soil which is similar to the movement of liquids. Rockfall is a very rapid failure of rock mass (Nemcok 1972). An overview of the common basic slope failure models was discussed by Poisel and Preh (fig.10). The following types of failure are considered to be of relevance for this thesis:

-Toppling means forward, valleyward directed rotation of blocks (fig.10i and 10j)
-Slumping refers to backwards, towards the rockface oriented rotation of blocks (fig.10d)
-Slope creep is a slow, continuous downward movement of rock mass or debris (fig.10k)
-Translational or rotational descent of blocks separated from in situ rock mass upon an incompetent layer, also known as “hard on soft” (fig.10f). This type is explained in detail in the following chapter.

Two or more types of slope movement when combined form a complex slope or mass movement. It is not always possible to classify all the individual slope movements (Hutchinson 1988).

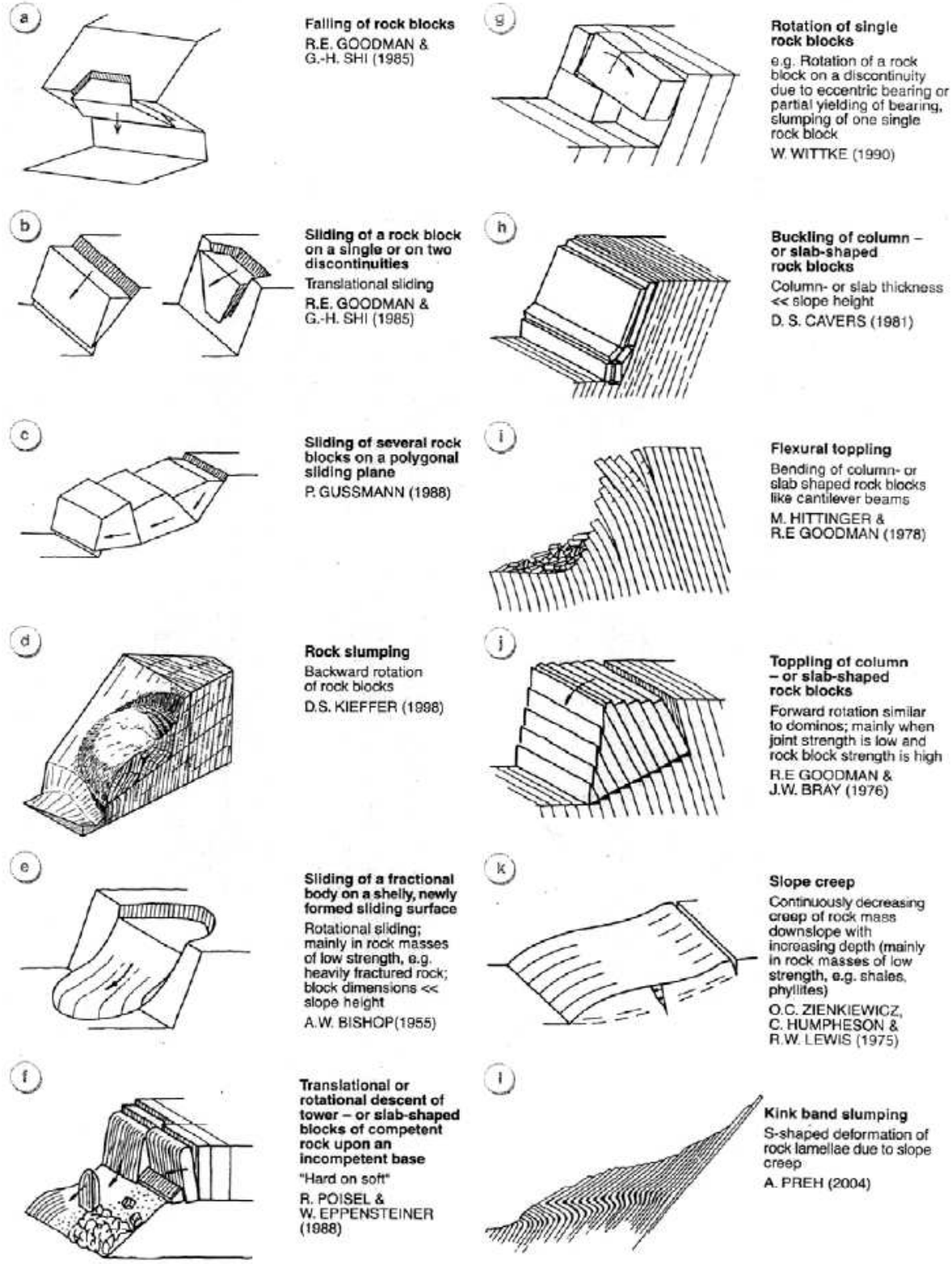

(fig.10): An overview of basic modes of failure at slopes and their mechanic behaviour (Poisel & Preh, 2004)

2.3.2 The System “Hard on Soft”

A competent layer of rock which is overlying a base of incompetent material (figs.10f and 11) is called a “hard on soft” system (Poisel, Eppensteiner 1989). Hard corresponds to brittle rock, soft means ductile material. Due to gravitation, the hard part starts to sink into the soft part, which reacts with an escape movement in the direction of free foreland. The result is a mass deficit, which causes the brittle layer to bow and finally break due to the induced stress. Friction constrains the escape movement of the soft layer, which causes horizontal normal tensile stress upon the brittle layer and leads to the formation of joints and fractures with both orthogonal and parallel direction to the border of the competent layer (fig.11) (Poisel, Eppensteiner 1989).

These fractures separate slabs and blocks from the brittle layer, if these blocks start to move downhill, three types of failure can be distinguished:

-translational movement of blocks (fig.11a)
-rotational movement of blocks (fig.11b and 11c):
    -toppling (fig.11c),
    -slumping (fig.11b)
-failure of ductile base (fig.11b) (Poisel, Eppensteiner 1989)

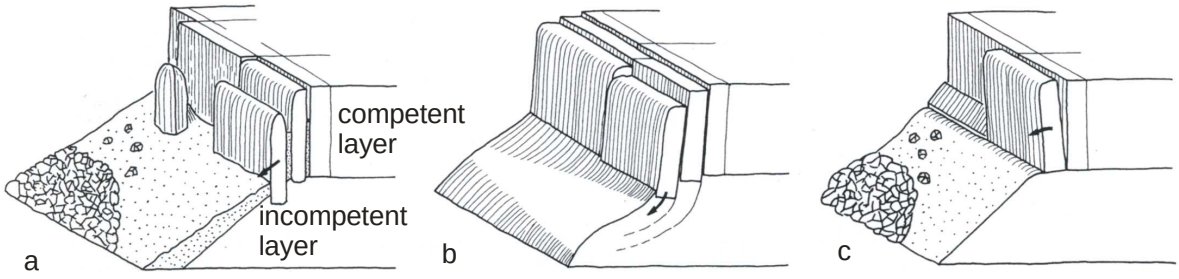

(fig.11): “Hard on Soft” System, a) translational descent of blocks, b) failure of soft base and slumping, c) toppling of blocks (modified after Poisel, Eppensteiner 1989)

Brittle deformation of the competent layer followed by separation and displacement of blocks commonly occurs along pre-existing tectonic discontinuities. During separation and movement of blocks, additional fractures can occur. Movement rates are in most cases very slow. Constant deformation rates, i.e. the lack of periods of faster deformation due to rainfall or other external factors, indicates creeping as the failure mode in the soft layer. The existence of both translational and rotational movement is a result of the absence of a

continuous gliding plane. Possible resulting mass movements, such as rock fall, can achieve much higher speeds than creeping (Glawe, Moser, 1989).

2.4. Structural Geology and Tectonics

Tectonic deformation at brittle conditions forms planar discontinuities without displacement due to lateral movement called joints, and discontinuities with apparent displacement called faults. Three main types of faults, normal faults (downward movement), thrust faults (upward movement) and strike slip faults, can be observed on scales ranging from centimetre to kilometre. Strike slip faults feature fault planes which are usually near vertical and the footwall moves laterally either left or right (Eisbacher 1996).

During strike slip, simple shear displacement within rocks produces characteristic fault structures that form at a specific angle to the main fault plane, called Riedel shear planes (fig.12). The dominant set, known as R shears, are synthetic and usually between 10° and 20° (or φ/2, φ is angle of internal friction) to the main fault trace. Secondary sets, the antithetic R´ and X shears form at about 70° (or φ - 90°) to the main fault. P shears are symmetric to R shears (φ/2) and Y shears parallel to the main fault. The P, X and Y shears are generally formed in later stages after R and R´ shears (Brosch, Kurz 2008, Meschede 1994).

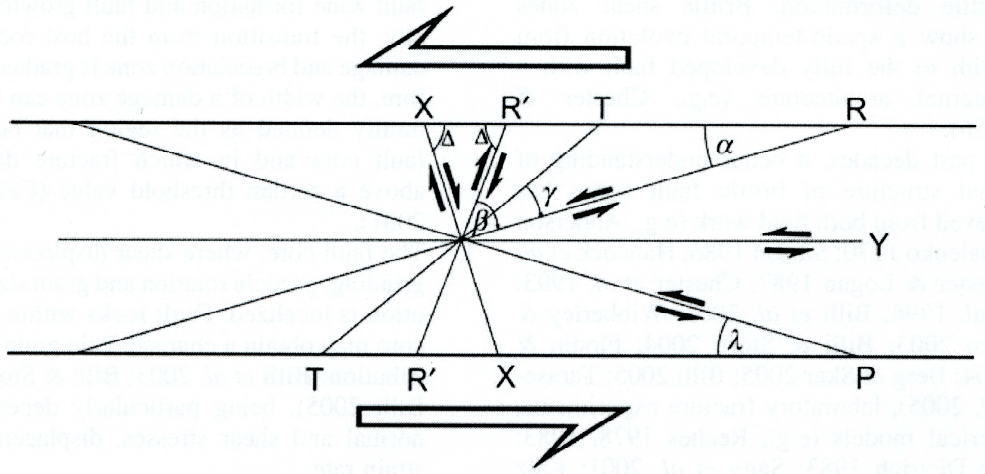

(fig.12): A schematic overview of Riedl shears planes and linked shears with their respective angles, α = λ = φ/2, β = φ - 90° (Kurz, Brosch 2008)

3 Methods

3.1 Field Mapping

Turiawald Plateau and its proximal foreland were mapped in 1:5000 scale. The western slope of the plateau was mapped in 1:2000. Additionally, two outcrops south of Turiawald, one at the village St. Ruperti and another one near the locality Oberdoerfl, were investigated. Mapping and further analysis was based on topographical (ÖK 205 1:5000, BEV 2005), geologic and hydrogeologic maps (KaGis Kaernten 2008, Poltnig et al. 2007), which were prepared by ArcGis. Mapping mainly focused on structural data of in situ rock mass at outcrops and selected inclined blocks on the slopes of Turiawald. The strike directions and number of depressions and sinkholes on the plateau itself were also mapped. When outcrop conditions allowed, bedding and jointing of blocks within the mass movement was also measured.

Outcrops were characterized by:

-size
-lithology
-bedding
-joints and fractures (Hancock 1984)
-brittle faults and slickensides (Meschede 1994) wherever possible with striation and sense of displacement
-duplex thrusts (Boyer, Elliott 1982)

Dip direction, dip of planes and striation were measured at outcrops. Strike of elongation was mapped at sinkholes and depressions on the plateau surface, as well as at mass movement blocks on the western slope of Turiawald.
The geological compass system Clar (360º degrees) was used as the mapping device. All stereographic plots presented in this thesis display dip direction and dip in great circle and pole plots. Rose diagrams depict strike directions.

The altitude and spread of the aquiclude along western Turiawald is of great importance to the springs in this area. To determine the position of the aquiclude (Langguth, Voigt 2004) in the working area, wetlands and outcrops of coal and fine clastic rocks on the western and northern slopes as well as tapped springs were mapped.

3.2 Structural Analysis

Computer aided analysis of structural data was carried out using several software programs:

Sphaira 2.0 (Porsche-Ully 2001) was used to plot bedding, duplexes and fault planes, which are displayed as great circles with their respective poles in a lower hemisphere stereonet (Lambert projection). Joints are plotted as poles and rose diagrams, lineaments as rose diagrams only. Statistical methods were used to calculate the centres of gravity of the different joint sets. Two small circles around the centre of gravity depict the spherical aperture and the cone of confidence (Fisher 1953). The vector of gravity is located within the cone with a probability given by the confidence limit. Calculations in this thesis were done using a confidence limit of 99%.

Fabric7 (Wallbrecher 2006) was used to plot slickensides and movement sense of striation. The orientation of paleo normal stresses was also calculated using *Fabric7,* using a paleostress determination method (Angelier, Mecheler 1977).

TectonicsFB (Reiter, Acs 2011) carried out correction of striation data for slickensides.

Stereo32 (Roeller, Trepmann 2003) computed density distribution of poles.

3.3 Analysis of Lineaments and Topography

Lineaments obtained by field mapping and from the digital elevation model of the overall topography of Turiawald and its surrounding forelands were analysed using *ArcGis 9.2,* which was also used to prepare and display mapping results.

Display and analysis of lineaments was done based on a digital elevation model with a raster spacing of 10 metres provided by Kagis Kärnten. Lineaments derived from this model and used in figures 21b and 24 were partly prepared and provided by Winkler et al.2006.
The Visual Basic macro *Polyline Angle* (Zazula 2005) was used to derive Azimuth angles from polylines drawn with *ArcGis.*

3.4 Hydrogeologic Monitoring

To determine the hydraulic behaviour and discharge volumes of the two investigated springs Roach and Pleier, as well as to obtain specific parameters such as electric conductivity and water temperature, data logging stations (data loggers type “Compact” by the company Logotronic) have been installed and maintained for a period of one and a half years for this project.

To calculate the discharge, the following procedure was carried out for the stations Pleier and Roach:

-recording the stage above the weir (every quarter of an hour) by pressure transducer sensor, which measures the combined pressure exerted on it by the atmosphere and the head of water above it
-measuring the temperature and electric conductivity (corrected for 25º C) by a multi parameter probe (every quarter of an hour)
-conversion of stage into discharge

To calculate water flow (total discharge) of Pleier Spring from stage records, analogue discharge measurements (stopwatch and bucket) were taken periodically to establish a stage discharge relation (potential function) and maintain a discharge rating curve. Each discharge measurement is correlated to the water level at the time the measurement was taken. With this information, discharge data can be interpolated and applied to the full range of water level measurements (Hölting, Coldewey 2005).

Because of high discharge volumes and the constructive form of Roach Spring as well as the fact that the spring was currently being used as a drinking water supply, it was not possible to perform analogue point measurements of water flow. To calculate discharge from water stages, the equation for sharp crested weirs with a rectangular control section was applied. Specific input data such as weir geometry measures was provided by Joanneum Research.

For comparison of the discharge rates, spring logging data from Roach and Pleier Springs collected by Joanneum Research in the years 2005 and 2006 (Poltnig et al. 2007) was analysed too. The precipitation on Turiawald for the time between the spring and fall of 2009 was recorded using an analogue ombrograph.

3.5 Theory of Discharge Analysis

3.5.1 Hydrograph

The discharge of a spring is described by the flow volume of water within a given time. This relation can be described by a hydrograph analysis, where the total discharge over a time period corresponds to the plane below the graph (Hölting, Coldewey 2005).

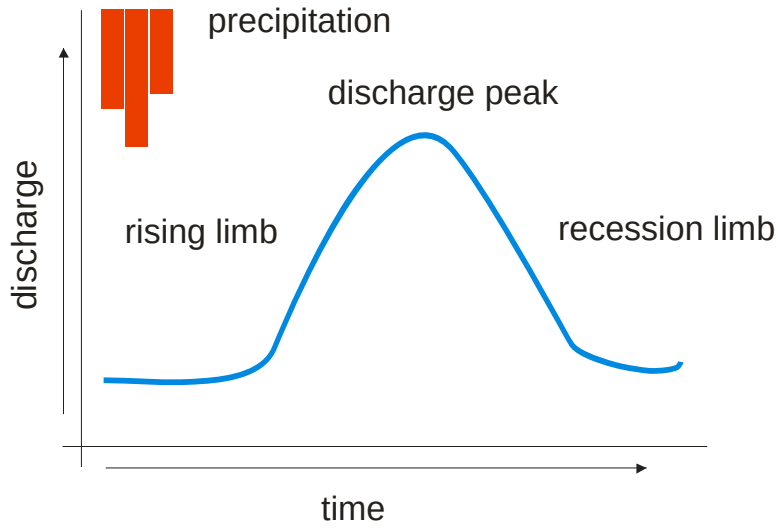

(fig.13): schematic hydrograph

Precipitation, which builds up water storage in the catchment area, leads to an increase in discharge, represented by a rising limb in the graph. The discharge peak is the highest point on the graph, when the greatest amount of water is discharged and the recession limb represents the withdrawal of water from the storage build up in the catchment area during earlier phases of the hydrograph (fig.13) (Kresic 2007).
Discharge is influenced by the amount of rainfall, or snowmelt in spring, infiltration conditions and the size of the catchment area, while the influence of precipitation on discharge depends on pore volume or jointing of the aquifer and the height of the groundwater table (Hölting, Coldewey 2005, Kresic 2007).

3.5.2 Quotient of Discharge

Simple discharge analysis can be done by calculating the quotient of discharge NQ/HQ (Hölting, Coldewey 2005), where NQ (l/s) is the lowest and HQ (l/s) is the highest discharge value over a specific time period. The arithmetic mean MQ (l/s) can also be determined.

Areas affected by karst formations are usually characterized by a fast and high infiltration rate of precipitation and a low surface runoff. Joints widened by dissolution in aquifers in carbonate rock provide high ground water flow rates. Therefore aquifers connected to karst formations have little storage capacity, variable discharge and a low quotient of discharge. Springs with small catchment areas show in most cases a fast reaction after precipitation events (Hölting, Coldewey 2005). The fast increase of discharge which is observable at karstified or strongly jointed aquifers is usually only a hydraulic reaction due to the rise of the hydraulic potential within the aquifer (Kresic 2007).

3.5.3 Coefficient of Discharge

Hydrographs can be used to make conclusions about the hydrogeologic conditions of the catchment area. During periods without rainfall, discharge decreases due to a lack of infiltration of precipitation water into the aquifer. The remaining discharge is called base flow. This part of the hydrograph can be used to make a base runoff recession curve (Hölting, Coldewey 2005), which can be expressed by an exponential equation (Maillet 1905):

$$Qt = Q0 \cdot e^{-\alpha \cdot \Delta t}$$

Qt [l/s] = discharge after time lag Δt (end of runoff recession)
Q0 [l/s] = discharge at t0 (start of runoff recession)
α [1/d] = discharge coefficient, specific for each spring
Δt [d] = time lag between Q0 and Qt in days (Δt = t - t0)

The discharge coefficient α depends on transmissitivity and storage capacity of the respective aquifer. The α values with an order of 10^{-2} imply fast discharge rates of well interconnected fissures or karst channels in the case of karst aquifers, while values of a magnitude of 10^{-3} represent slower discharge from aquifers of small voids like narrow fissures and joints (Kresic 2007). If the hydrograph is displayed as a logarithmic graph, and no serious disturbances like rapid water inflow is present, the discharge coefficient corresponds to the inclination of the recession straight line. Different inclinations usually represent different discharge micro regimes. The discharge coefficient α is calculated by the following equation (Maillet 1905):

$$\alpha = (log\ Q0 - logQt) / (0{,}4343 * \Delta t)$$

0,4343 = conversation factor to express discharge in volume per time

The coefficient of discharge allows the prediction of discharge after any given period of time. In addition this coefficient can be used to calculate the theoretical total amount of groundwater accumulated in an aquifer at the start of a recession period, which is explained by the following equation (described e.g. in Kresic 2007):

Vt = Qt / α

Qt = discharge at time t

Vt = Volume of accumulated water above level of discharge

Springs draining karstic or highly permeable jointed aquifers often have two or three micro regimes of discharge. These regimes are described by discharge volumes and their respective alpha values, which indicate different porosities and storage capacities within the aquifer as explained above. The corresponding volume of groundwater stored in the aquifer at the beginning of the recession is the sum of the different volumes. The following equation is assumed for three volumes (fig.14) (Kresic 2007):

V0 = [(Q01-Q02)/α1))+ (Q02-Q03)/α2)+ (Q03/α3))] * 86400

V0 = total amount of groundwater stored at the start of a recession period

Q01 to Q03 = discharge (l/s) at the beginning of recession, see figure 14

86400 = factor to convert days to seconds

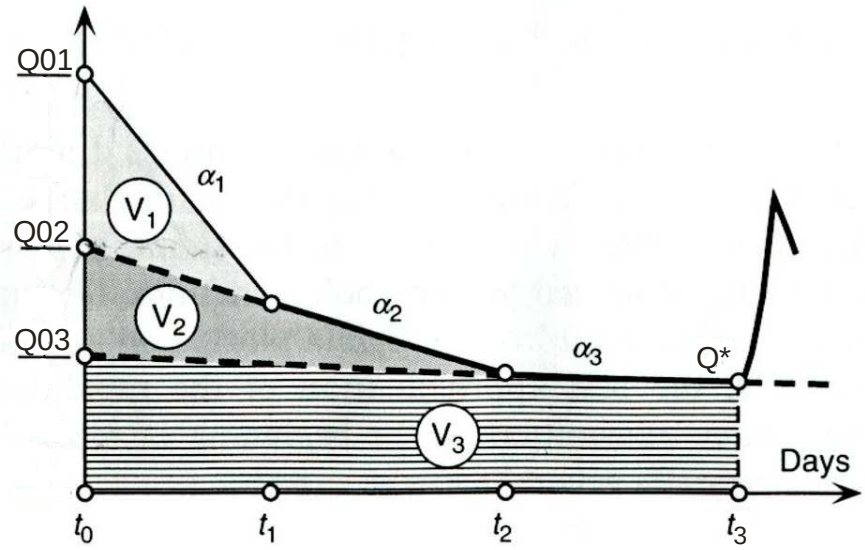

(fig.14): A schematic graph of recession with three micro regimes and their respective volumes and α values (modified after Kresic 2007)

3.5.4 Natural Tracers

During the recharging of groundwater in karst systems, marked by a rising limb on the hydrograph, variations of the electric conductivity of the water can take place. At first, often after a long period without rainfall, the electric conductivity shows a short initial increase at the beginning of the increase of discharge, which represents old, highly mineralized subcutaneous water (water stored close to the surface, interacting with soil CO2 and carbonate rock) being flushed out by the hydraulic pulse (fig.15). Then the electric conductivity decreases rapidly, since chemical reactions between recharge water and carbonate rocks are very fast (hours to days). Every deviation from background conductivity and temperature levels can be interpreted as water moving rapidly though the aquifer. Another explanation for the decrease in electric conductivity of the water is a dilution effect by the mixing of freshly infiltrating water with the longer stored and higher mineralized water (Sauter 1992).

Time lags of discharge and conductivity peak values are an important criterion for quantitative analysis. They reflect the speed of response of the aquifer to infiltrating water and reveal transit times of the water through the conduit system (i.e. joints and fractures). The time difference between the maximum increase of discharge (arrival of fresh water maximum at the water table) and the minimum peak of electric conductivity (arrival of new water at the spring) is assumed to be the time for the transit of the water through the conduit system of the aquifer (fig.15) (Sauter 1992). Springs draining karstified or intensely fractured aquifers can react in hydraulic means within hours to a precipitation event (Kresic 2007).

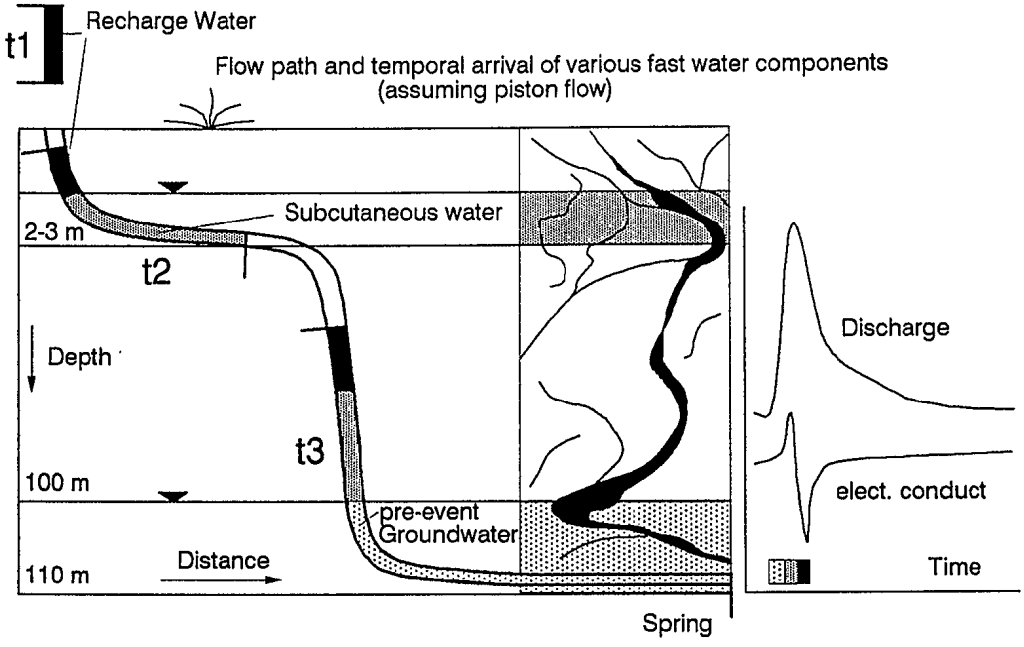

(fig.15): flow path and change in spring water parameters due to recharge water (Sauter 1992)

4 Results

4.1 Structural Geology

4.1.1 Outcrop St.Ruperti

South of Turiawald at the location St.Ruperti (fig.23), an outcrop is located, where strongly fractured and faulted, gray coloured marbles are exposed. The bedding dips about 70º to the south (fig.17a). Four main joint sets (fig.17b and 17c) can be distinguished, one approximately N/S striking steeper set (dip about 70º to 80º), one set with NW/SE strike (dip 80º) and two NE/SW striking sets (dip between 40º and 70º). Almost no or only in [mm] scale opened apertures separate the joint planes.

Several forward propagating duplex thrusts (fig.17f and fig.16) intersect joints and show mainly NE/SW striking flats and ramps. The transition bend from flat to ramp is often characterized by cataclastic rock. Faults (fig.17d) intersect both duplex thrusts and joints, mostly filled with cataclastic material. At two spots the marble has been worked up to a bright gray fault breccia, weathered and covered with a yellow to brownish coating.

Slickensides (fig.17g) are nearly striking to N/S and ENE/WSW, striation mainly shows thrusting in NW to NNW direction and sinistral W/O oriented strike slip faults. Reconstruction of paleo stress elipsoid shows as principal normal stresses σ1: 211/36, σ2: 111/16 and σ3: 002/57 (fig.17g).

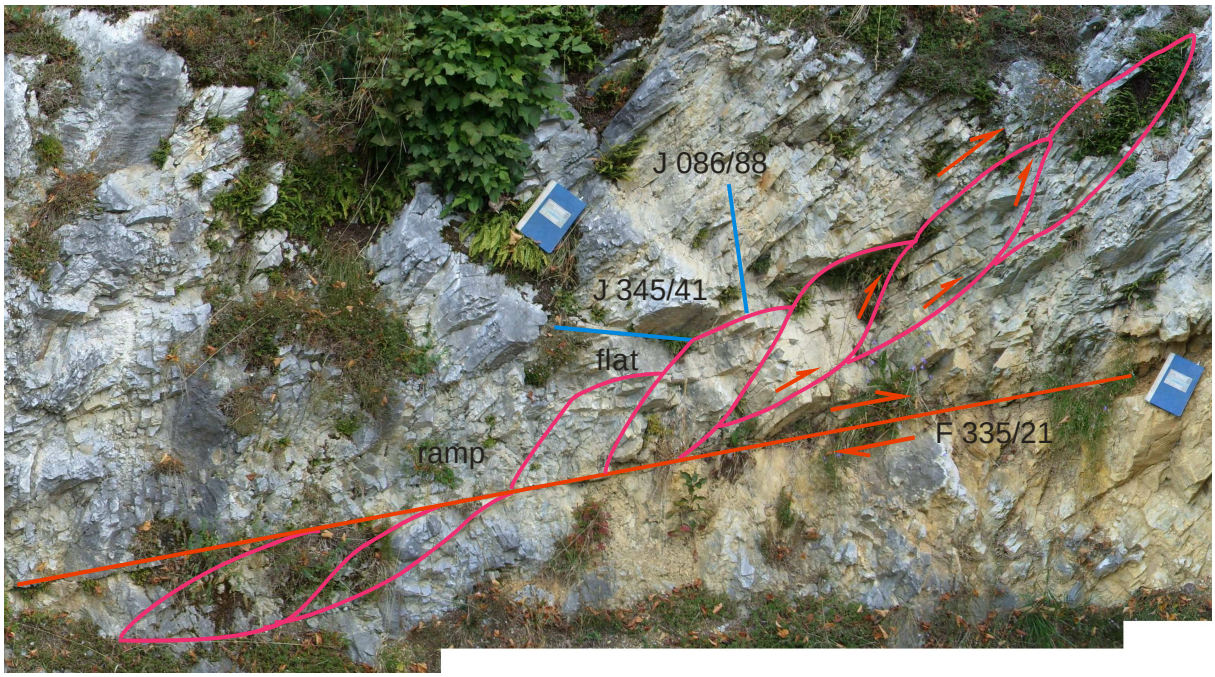

(fig.16): outcrop St.Ruperti, red: fault (F), pink: duplex thrusts with respective ramps and flats, blue: joints (J),

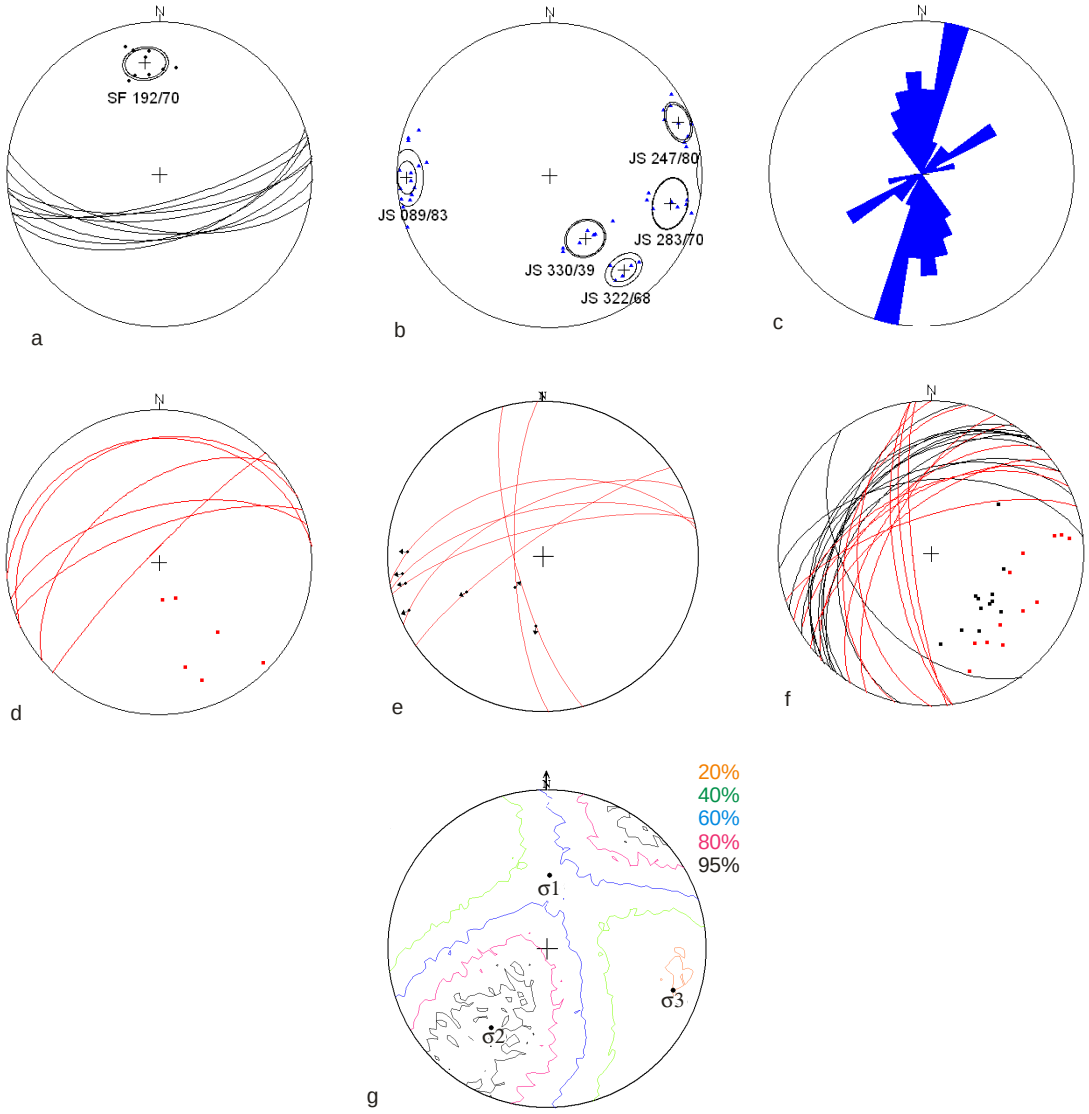

(fig.17): Lambert projection with structural data outcrop at St.Ruperti: a) bedding (great circles and poles); b) joints (poles with centers of gravity); c) joints (rose diagram); d) faults (great circles and poles); e) slickensides (great circles); f) duplex thrusts (great circles and poles, black: flat; red: ramp); g) paleo stress analysis and principal normal stress

4.1.2 Outcrop Oberdoerfl

Another outcrop south of the plateau is situated about one kilometre east of St.Ruperti near the village Oberdoerfl. Again a gray, fractured calcitic marble is exposed, although less tectonically stressed but heavily weathered. Structural data is similar to St.Ruperti. Bedding dips 50º to the south (fig.18a), three joint sets (fig.18b and 18c) are present, two nearly corresponding to the St.Ruperti outcrop striking approximately NW/SE and SW/NE with an almost vertical dipping, and one other more flat dipping set striking NW/SE (dip 39 º).

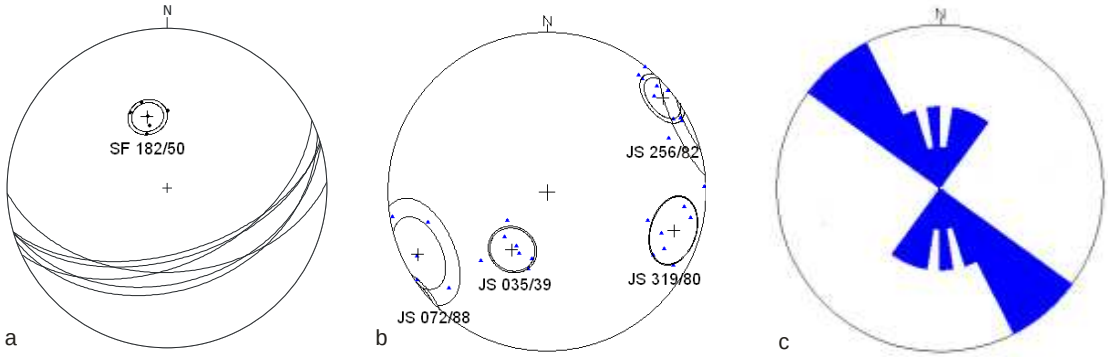

(fig.18): Lambert projection with structural data, outcrop Oberdoerfl: a) bedding (great circles and poles); b) joints (poles with centers of gravity); c) joints (rose diagram)

4.1.3 Turiawald Rock Faces

The Sattnitz Conglomerate of Turiawald is exposed at the plateaus up to 100 metres high, almost vertical rock faces, especially at the northern, western and eastern flanks. It is mainly horizontally layered (fig.19a) and shows almost no weathering or dissolution effects. At least three approximately vertical joint sets (fig.19b and 19c) can be found all around the plateau. Predominant strike directions are N/S to NW/SE and W/E.

Open joints appear frequently at the edge of the north western and western flank. On the foot of the rock faces the joint aperture is mainly in [cm] scale, at the crest, especially in the north west, many joints are widened up to metre broad joint openings (fig.23). The strike of these joint openings is mainly N/S. The strike of joints sets is in most cases approximately perpendicular or parallel to the rock faces of Turiawald (fig.23, 19c and 21b).

At several sites along the northern western face, blocks can be found, which are almost removed from the plateau but still have contact to the in situ rock mass, as well as blocks

which are already completely removed (fig.28). The inclination of their joint planes parallel to the faces suggests slumping and toppling as future modes of failure (fig.19d), once the block is finally removed from the rock face.

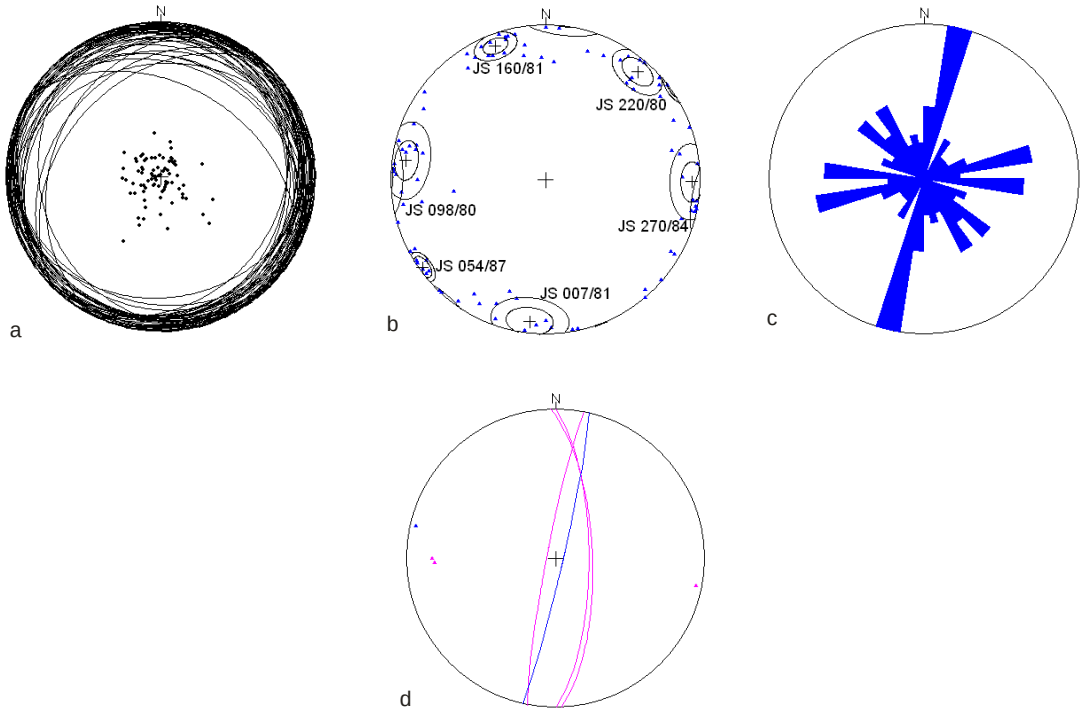

(fig.19): Lambert projection with structural data, rock faces of Turiawald plateau: a) bedding (great circles and poles); b) joints (poles with centres of gravity); c) joints (rose diagram) d) vertical joints (pink) and average face (blue) (great circles and poles)

(tab.1): Summary of structural data (centres of gravity of the bedding (SF/SS) and the joint sets (JS)) of the three compared outcrops. Numbers of joint sets do not represent ranking of formation time of joint sets

	plane set	SF/SS	JS1	JS2	JS3	JS4	JS5	JS6
domain								
St.Ruperti		192/70	247/80	283/70 089/83	322/68		330/39	
Oberdoerfl		182/50	256/92 072/88		319/80			035/39
Turiawald		166/13	220/80 054/87	270/84 098/80		160/81 007/81		

The joint set JS1, which occurs at all three of the investigated outcrops St.Ruperti, Oberdoerfl and the rock faces of Turiawald plateau, shows similar orientations (tab.1 and figs.17, 18, 19). The difference between dip directions at the respective outcrops is between 10º and 25º, the respective dip angles show differences of approximately 10º (tab.1). Joint set JS2 appears at St.Ruperti and Turiawald outcrops. Differences in dip directions and angles are around 10º (tab.1 and figs.17,19). At the sites St.Ruperti and Oberdoerfl JS3 appears showing approximately equal dip directions and dip angles with a difference of about 15º (tab.1 and figs.17,18). Joint sets JS4, JS5 and JS6 only occur at their particular outcrops (tab.1 and figs.17,18,19). The correlations between these joint sets indicate that their formation is caused by the same driving forces.

4.2 Geomorphology

4.2.1 Regional Lineaments

Analysis of the digital elevation model of the Klagenfurt Basin around the western Sattnitz Mountains and their foreland revealed the existence of several lineaments which feature iterative strike directions, such as terrain edges, lake coastlines, valleys and rivers. Four predominant strike directions can be identified: N/S, W/E, NE/SW and NW/SE (fig.20).

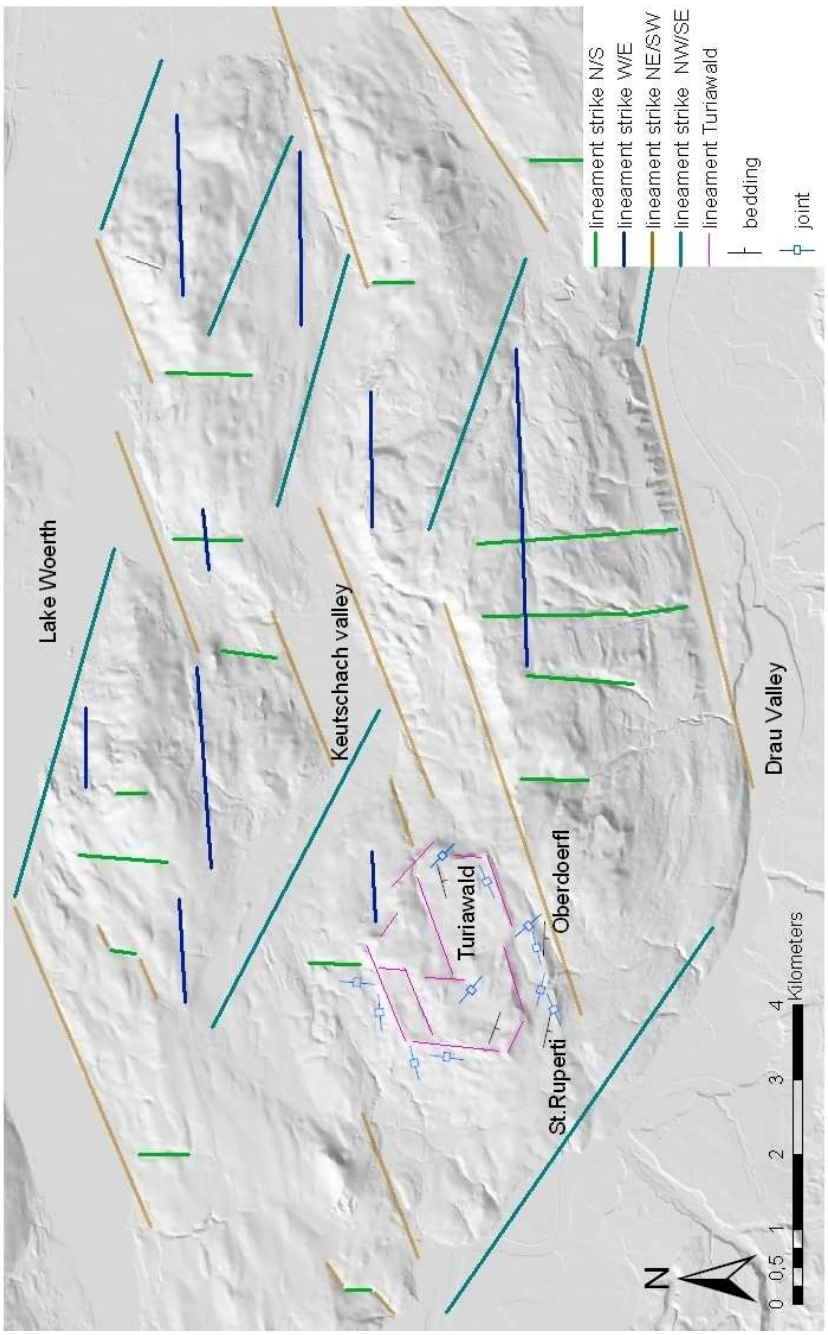

(fig.20): DEM of the western Sattnitz Mountains and Turiawald with its foreland in scale 1:60000, main regional lineaments of this area and corresponding lineaments of Turiawald, as well as bedding and joint sets of the investigated outcrops with strike directions correlating to lineaments

The lineaments shown in (fig.20) have been selected because of their recognisability on the DEM (resolution 10 metres) and a minimum elongation of 0.5 kilometres.
These lineaments (fig.22) correlate roughly with the strike of the respective joint sets which can be found at the outcrops St.Ruperti, Oberdoerfl and Turiawald rockfaces (fig.20 and 21a), as well as with the main strike directions of lineaments on the Turiawald plateau (fig.20 and 21b, see also fig.24).

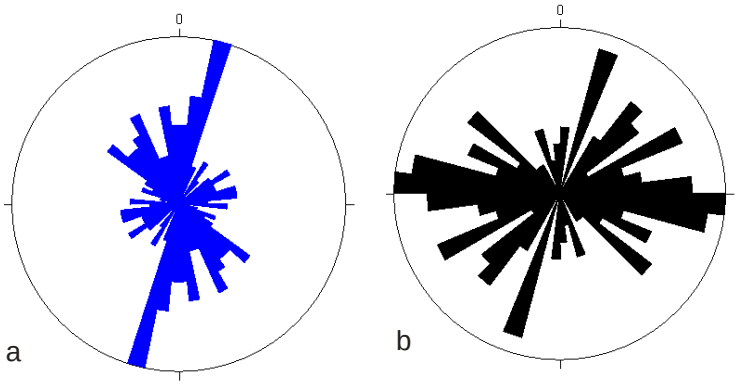

(fig.21): Lambert projection with structural data a) strike directions of joints from the investigated outcrops, b) overall lineaments of Turiawald

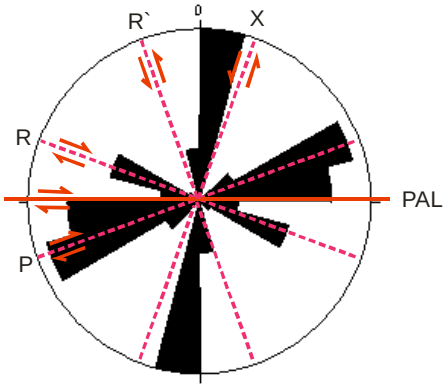

(fig.22): Lambert projection with structural data, N/S, W/E, NE/SW and NW/SE lineaments shown in (fig.20), ideal Riedel shears (R), ideal P shears (P), ideal R´ shears (R`) and ideal X shears (X), Periadriatic Line (PAL)

Assuming that the large scale lineaments mentioned above (fig.20) have been formed due to deformation along the Periadriatic Line, it is possible to correlate them in kinematic ways. The lineaments which are striking NW/SE are at an angle of about 12º to the Periadriatic Line and can therefore be seen as Rieldel shears (fig.22). Lineaments striking in a NE/SW direction are at an angle of 14º to 19º to the Periadriatic Line and can be understood as the linked P shears of the fault line (fig.22). N/S striking lineaments (75º to 90º) are close to the ideal angle of R´ and X shears (fig.22), while W/E striking lineaments can be seen as Y shears parallel to the PAL or as glacial phenomena (fig.22).

4.2.2 Turiawald Plateau

Mapping on the Turiawald plateau itself was mainly focused on sinkholes, cracks and wetlands. Due to glacial overprint during the last great ice age, outcrops for obtaining structural data (bedding, joint sets) can only be found in very small numbers.
Sinkholes (fig.23), cracks and crate like depressions occur frequently on the western, north western and eastern part of the Turiawald plateau (fig.25). In bigger numbers they can be found within its boundary area, but also in a distance of up to 1 kilometre from the plateau margins, mostly in the north western part (fig.26). The strike direction of these small scale lineaments is in most cases parallel or roughly orthogonal to the escarpments, and also correlates with strike of large scale lineaments and joint sets.

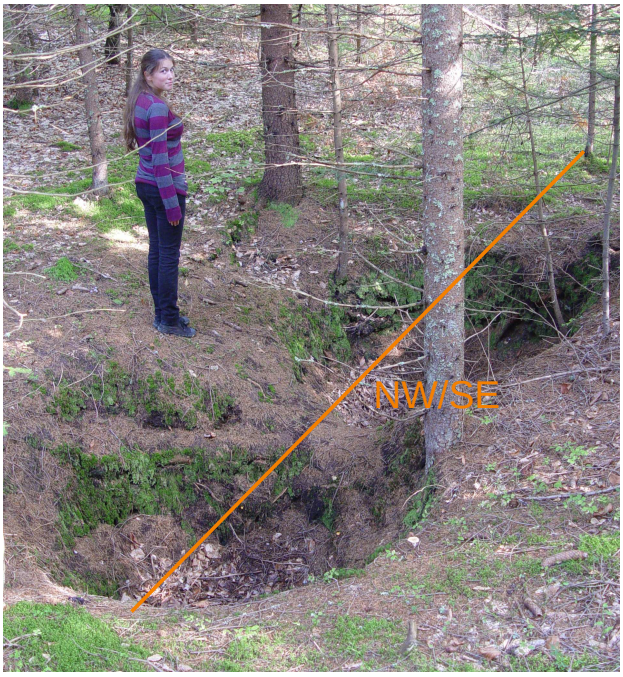

(fig.23): Adjacent sinkholes, line shows strike direction

The sinkholes have in most cases a diameter of about two metres. Usually groups of such holes can be found next to each another, often arranged in a row like beads (fig.23 and fig.26). The strike directions of these rows as well as the elongation of single holes are mainly oriented in W/E and NE/SW to NW/SE directions (fig.23 and fig.24a). These orientations are approximately parallel to the strike of joint sets as well as to the strike of large scale lineaments (terrain edges, elongated depressions etc.) and plateau margins (fig.19c, fig.24, and fig.26). The south western and eastern areas show smaller numbers of such small scale depressions (fig.25). In the central area of the plateau, almost no small scale sinkholes can be found, but the digital elevation model shows two roughly elliptic shaped large scale depressions almost in the centre of Turiawald and two lowered areas in

the south western and north eastern parts of Turiawald (dashed envelopes in fig.25). Turiawald shows generally an undulatory morphology.

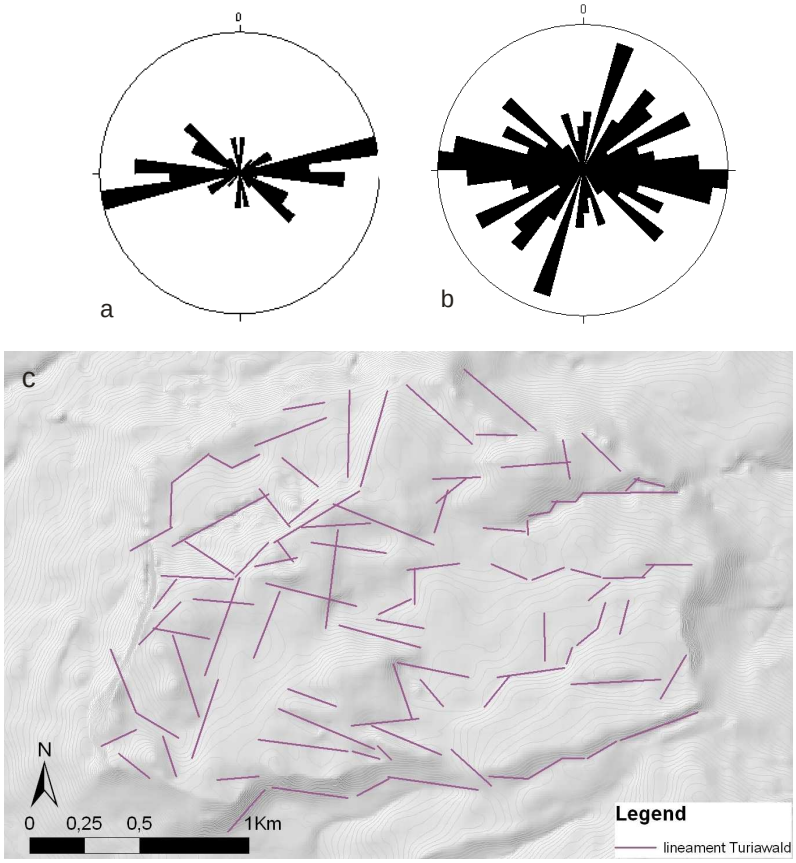

(fig.24): a) strike of sinkholes; b) overall lineaments (plateau edges and lineaments derived from DEM); c) DEM of Turiawald plateau with lineaments (modified after Winkler et al.2008)

Analysis of the digital height model shows a step-like decrease in the topography elevation of the Turiawald plateau from south east to north west.
The south easternmost flank of the plateau has a height of about 880 metres above sea level, and the central area is roughly 800 metres high. In the northwest, the plateau has only an average height of 730 metres (fig.25). The boundaries of the elevated and the sagged slabs (dashed lines in fig.25 and fig.26) have approximately the same orientation as the strike directions of joint sets, sinkholes and lineaments of Turiawald rock faces, mainly in NE/SW direction (fig.24 and fig.26).

At the north western sagged slab, the most fractures, joints and sinkholes appear. The orientation of their strike is usually roughly parallel or perpendicular to the tear off edges of the plateau in this area (fig.26). A significant number of joint openings appear here, mostly striking N/S (fig.26). Lineaments are considered to be of extensive character, due to the aperture of joint openings and sinkholes.

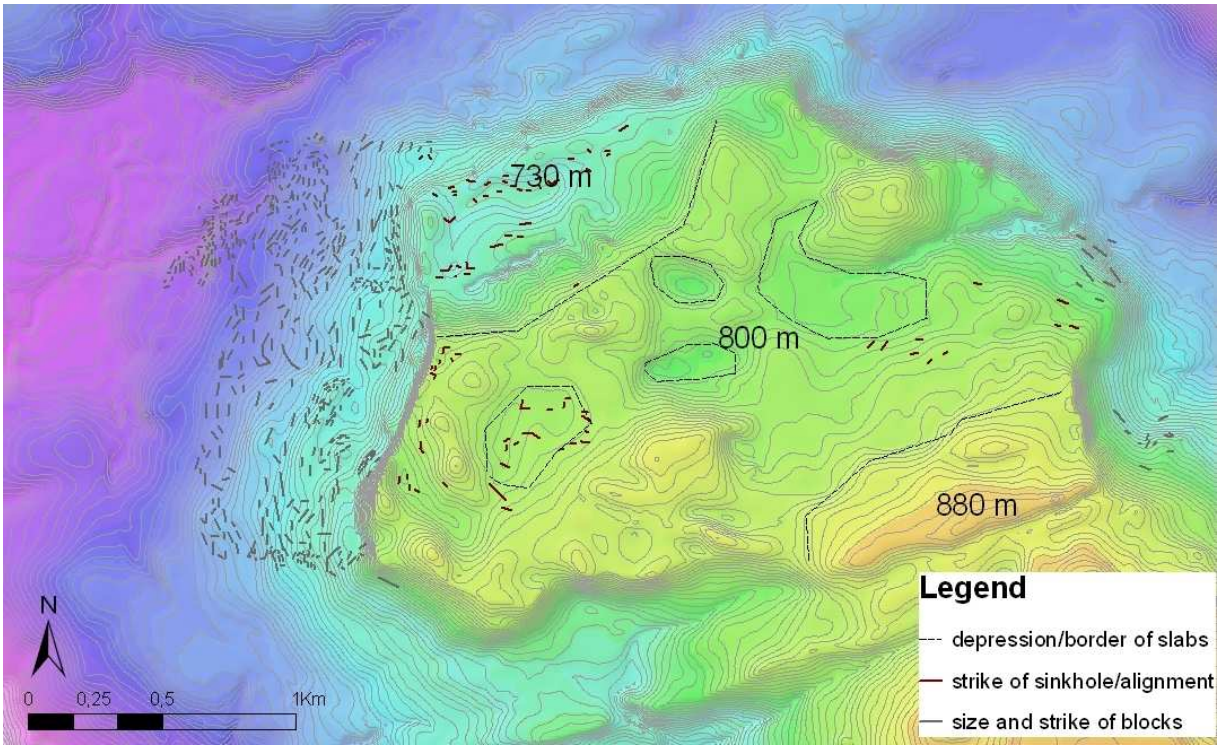

(fig.25): DEM of Turiawald average height distribution in m.a.s.l., colours illustrate elevation: orange/yellow to bright green = 880 to 830 m, bright green to green = 830 to 750 m, green to turquoise = 750 to 700 m, lowermost north western part (730m) is also shown in a smaller scale in figure 26

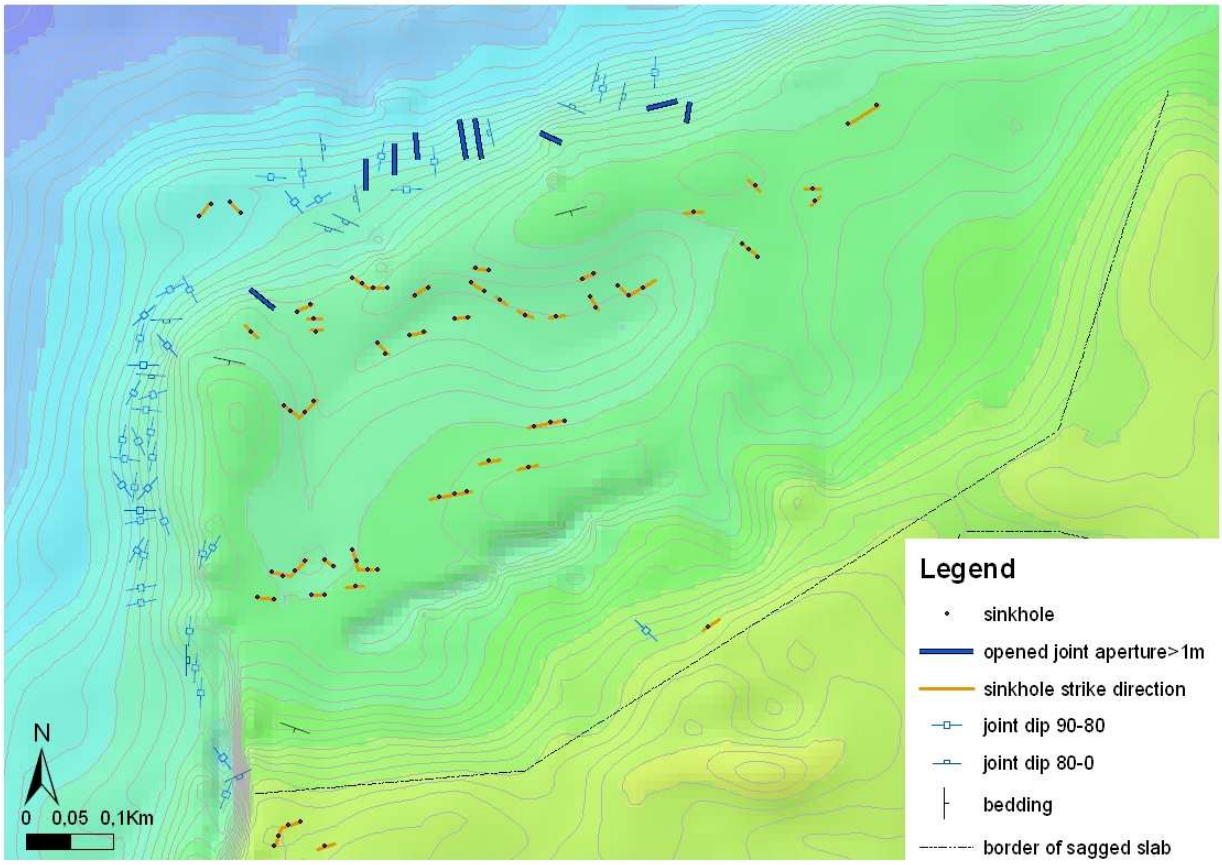

(fig.26): DEM of north western flank of Turiawald; sinkholes and their respective strike direction, bedding, joints and joint openings.

4.2.3 Turiawald Western Slope

The western slope of the investigated plateau shows an undulatory topography of wall and trench structures. It is characterized by a mass movement, which consist of blocks that have been separated from the plateau and are moving down the slope, supported by a matrix of conglomerate debris. The total mass movement area derived from the DEM is approximately 2.9 square kilometres.

Block sizes range from lengths of several metres up to 170 metres long and appear in an elongated, rampart like form. From north to south, the number of blocks decreases, while the overall length of the blocks increases (fig.27 and fig.30). The strike of the elongation of blocks is roughly parallel to the contour lines of the surface topography and the plateau's tearoff edges (fig.30). The northern part of the mass movement is characterized by blocks that are smaller in length and shorter in height. In comparison, the southern mass movement area contains several tower shaped blocks that can be found standing upright. The maximum number of blocks of the investigated area can be found above Roach Spring, which are also relatively small in height and length (fig.30).

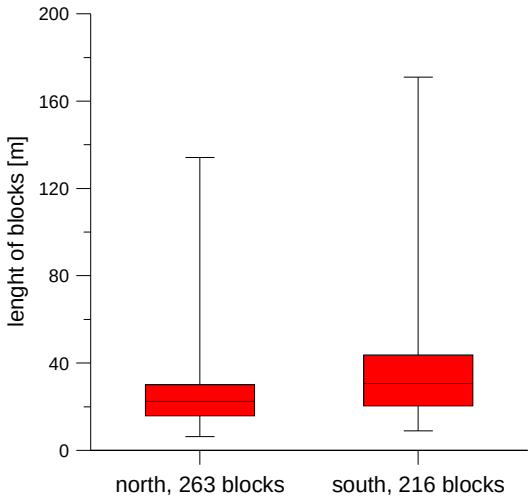

(fig.27): Number of blocks at the northern and southern areas of Turiawald's western slope in relation to average (red block) and overall length (black line)

The western slope shows a convex topography. Elevation difference between the head and toe of the mass movement body is about 180 metres, while the distance between the head and toe is about 1.2 kilometres long. The slope has an average inclination of 10º.

During field investigations it was observed that the transition to the margin of the mass movement on the western slope is indicated by a termination of block and mass movement bodies and a more even topography (fig.30). On the northern and southern foreland of the Turiawald plateau, the number of blocks sharply decreases from west to east and the topography becomes less undulous. Only at the easternmost slope can a few blocks be found which are of similar appearance to those on its western slope counterpart (fig.25). These blocks already belong to the Dobein mass movement (Fellner 1993). The border of the mass movement is significantly different when derived from the DEM according to convex topography markers (fig.30).

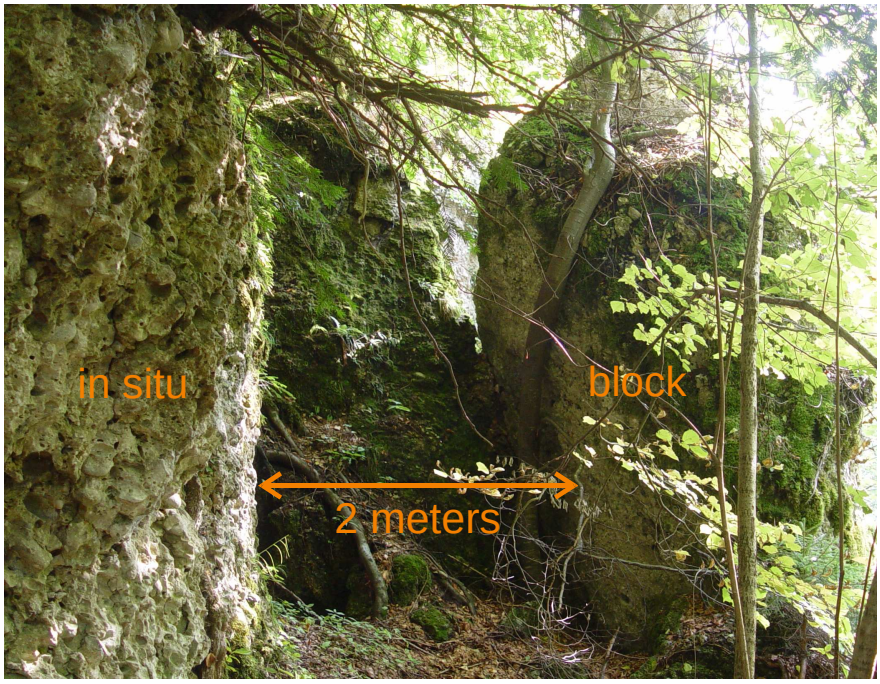

(fig.28): Block removed from in situ rock mass at the western slope of the Turiawald plateau

Debris from the plateau can be found as filling material between the blocks all over the mass movement area. At two locations debris from recent rock falls can be found directly at the foot of the rock faces (fig.30). Coal beds and fine clastic rocks outcrops can be found in contact with conglomerate blocks at three sites (fig.30). Both coal and conglomerate blocks show the same structural orientation.

Along the western slope, several tilted blocks are situated within a few metres of the in situ rock faces (fig.28). Their tilt angles, as well as varying dip angles of the nearly vertical faces and inclination of blocks still in contact with the face (fig.19d), indicate both rock slumping and rock toppling as mechanisms of failure.

To verify the assumed slumping and toppling failure of blocks, the structural data obtained from field mapping was analysed using stereographic projections. Blocks on the northern area of the western slope, which are close to the rock walls, show a mainly forward rotation indicating toppling failure (fig.29a). Translational movements and slumping of blocks (fig.29a) occur less often. Blocks which are at a minimum distance of 500 metres from the escarpment show mostly slumping and some translational movement, but almost no toppling (fig.29a).

The southern area of Turiawald's western slope shows less activity in block movement and rotation. Dip angles of blocks close to the rock face as well as of blocks more far away show about the same relatively small values (fig.29b). Almost the same types of movements of blocks occurring in the northern area also occur here. The little variation of bedding data values indicates much less intense movement and rotation (fig.29b)

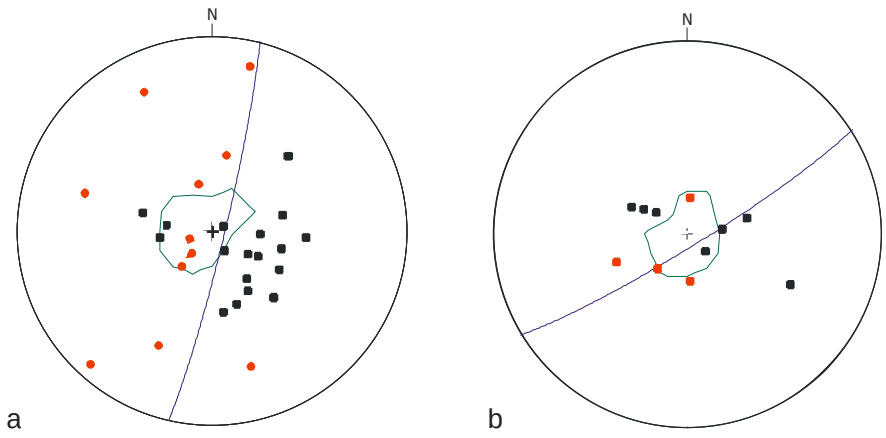

(fig.29): Lambert projection with structural data, a) northern part of western slope, b) southern part, great circle = face, green envelope is limit of in situ bedding (minimum density distribution of pole points), black poles = bedding of blocks within 10 m of face, red poles = blocks within about 500 metres distance of face

Several underground and open pit coal mines are known to be in this area. An adit to an abandoned coal mine ("Augustistollen") is located close to the escarpments (fig.27). The gallery strikes W/E into the mass movement. During the time from the spring to the fall of 2008, this gallery was affected by three cave-in events. Further investigation was stopped due to anticipated danger of continuing roof falls. The observed material inside the gallery was unconsolidated conglomerate debris ranging in size from [cm] gravels to [m] blocks. On some spots on the roof, precipitation of thin layered speleothem can be found.

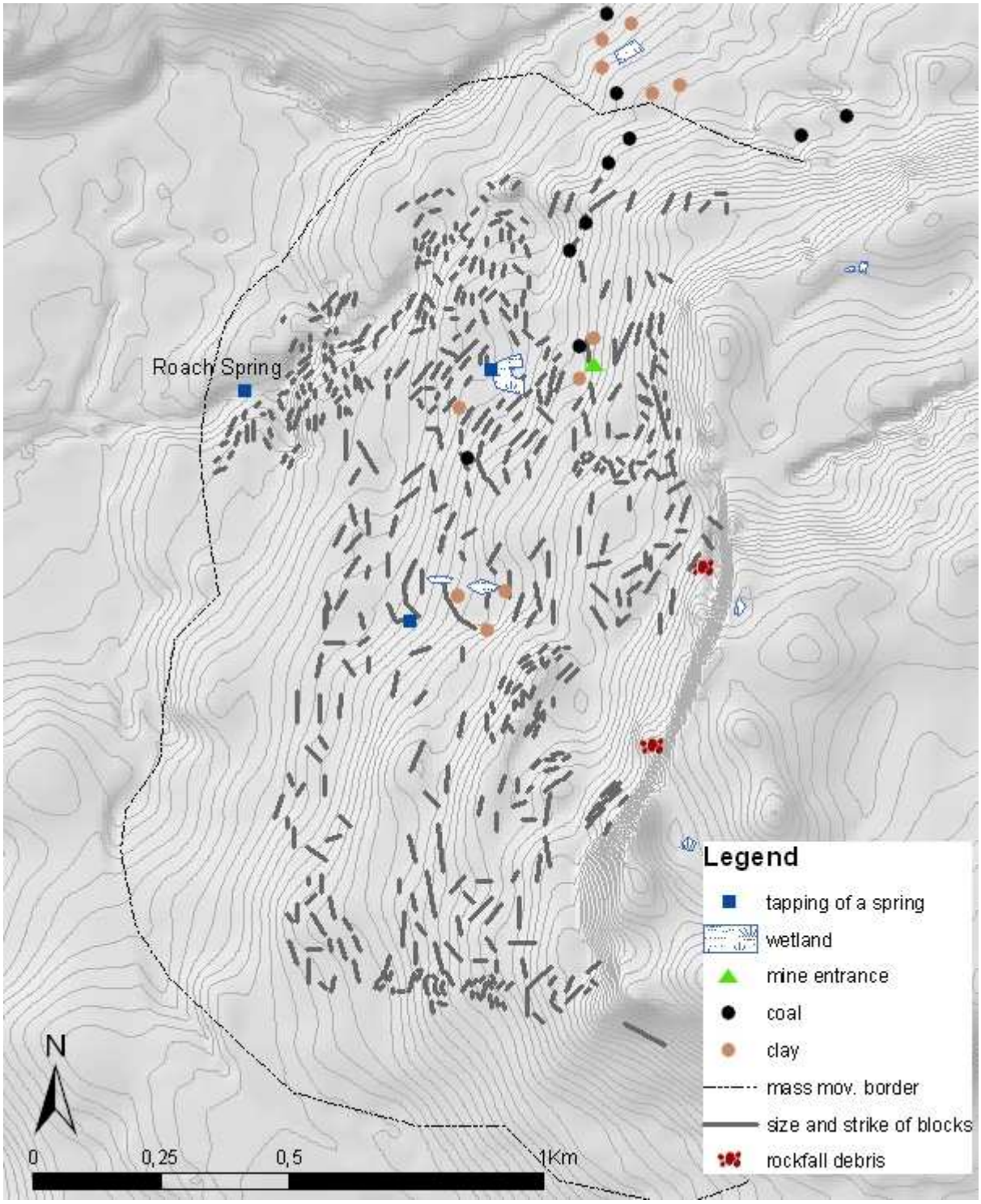

(fig.30): Turiawald western slope mapping results, the western border of the block field on this map is also the border of the mass movement body

4.3 Hydrogeology

4.3.1 Hydrogeologic Mapping

To find the uppermost limit of the aquiclude in the mass movement area on the western flank of Turiawald, the occurrence of the basal fine clastic rocks of Penken Formation in this area was a major target of the mapping campaign for this project. Since coal deposits are interbedded within the clastics, they were also mapped. Wetlands, suspicious vegetation, tappings of springs and other signs of groundwater daylighting were also of interest.

Several outcrops of coal and fine clastic rocks, two tappings of springs and three wetland areas (fig.30) can be found on the northern part of the western slope, mainly occurring between 610 and 660 metres above sea level. The entrance to an abandoned coal mine can also be found here (fig.30). The southern part of the western slope did not show any of these features.
On the Turiawald plateau itself only some minor wetlands have been found, no surface flow of water was present.

A NE/SW striking lineament forms a small valley which is cut into the western slope, which is also where Roach Spring is located, almost at the deepest point of the mass movement (fig.30).

4.3.2 Aquiclude of Western Turiawald

The height difference between the verified position of the aquiclude trace on the southern escarpment, and springs or wetlands (except Roach Spring) on the western slope is an average of approximately 140 metres. This indicates an average dip angle to the northwest for the aquiclude of about 4.5 degrees below the mass movement and western Turiawald.

Considering this information together with the mapping results (outcrops of fine clastic rocks and coal, tappings of springs, wetlands, see figure 30) and known positions of coal and fine clastic rocks on the north western slope, the position of the aquiclude bed can be located in the area between the contour lines of 630 and 660 metres above sea level, illustrated by the hypothetical trace of the aquiclude (fig.31). This assumption can be made for the northern part of the western slope.

Due to the lack of outcrops of fine clastic rocks and coal or signs of water on the surface of the southern area of the western slope, the run of the aquiclude in this area was interpolated by overlapping its dip angle with the topography. Therefore the supposed run of the aquiclude is similar to the verified trace on the southern slope of Turiawald, but moved about 30 metres downhill, and can be located at an altitude of approximately 645 metres as shown in figure 31.

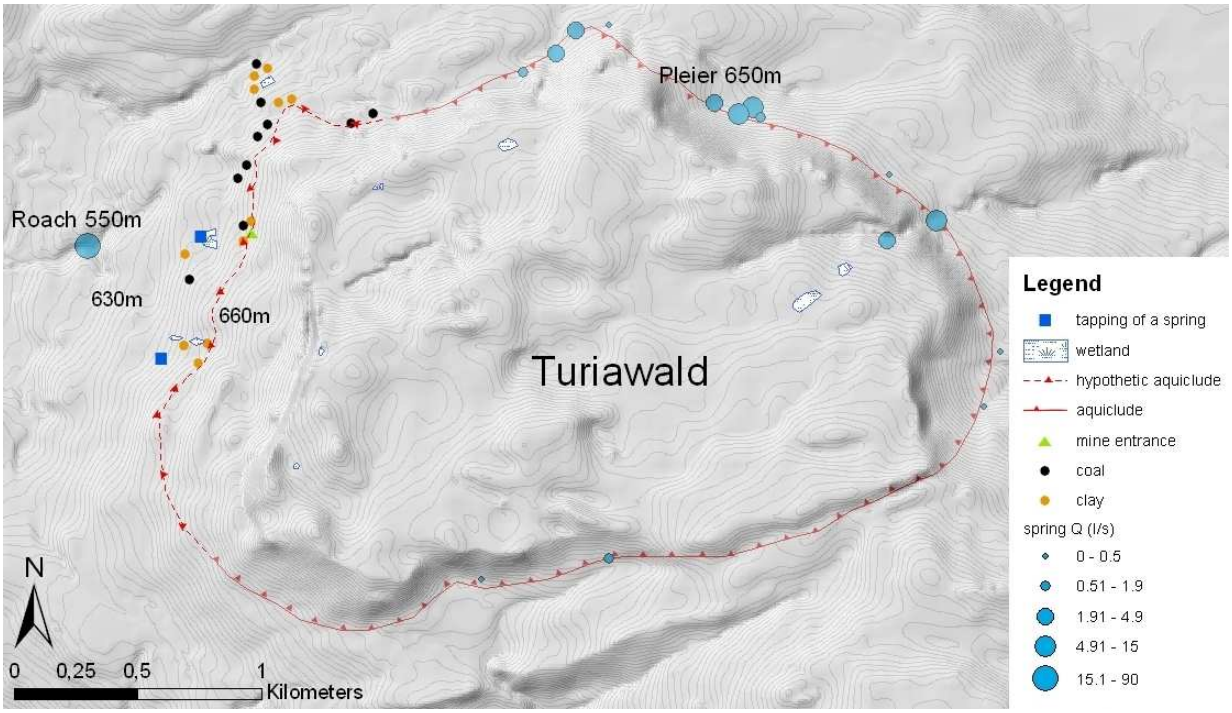

(fig.31): run of the hypothetic aquiclude on the western slope of Turiawald

4.3.3 Hydrogeologic Monitoring

Water stage recordings by data loggers have been converted to discharge by the weir equation for Roach Spring. For Pleier Spring the following discharge rating curve (fig.32) has been derived from stage / discharge relation:

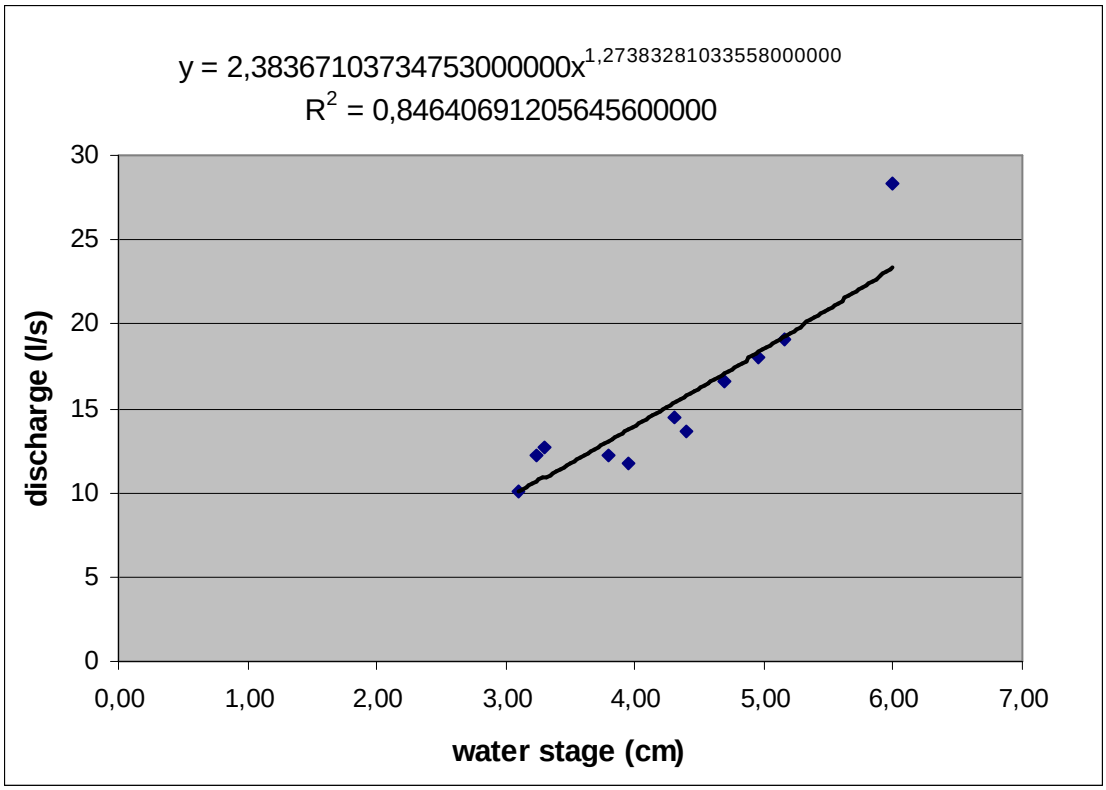

(fig.32): Pleier Spring discharge rating curve and its respective power function

Due to weir geometry (two spillovers of different size) and a relatively small head above the crest, the conditions to maintain an ideal rating curve were not perfect.

Pleier water inflow consists of three spring tappings and the overfall from the Hojoutz water gallery, which flow into a collecting basin.

The Pleier and Roach Springs show strongly different maximum and average discharge rates. Minimum discharge values, however, are approximately the same. Both springs show similar electric conductivity and temperature (tab.2).

(tab.2): mean values of discharge (Q) from summer 2008 to summer 2009, electric conductivity (EC) and temperature (T) from the Pleier and Roach Springs

	Q min (l/s)	Q max (l/s)	Q ø (l/s)	EC min (µS/cm)	EC max (µS/cm)	EC ø (µS/cm)	T min (ºC)	T max (ºC)	T ø (ºC)
Pleier	9,37	20,83	13,03	306,95	316,04	312,18	7,50	8,17	7,9
Roach	9,17	402,85	99,31	296,39	321,16	310,1	7,81	8,04	7,9

Roach Spring has a lower quotient of discharge NQ/HQ, but a higher average discharge rate MQ. Minimum NQ, maximum HQ and mean MQ values for both measuring points are presented in the following table (tab.3):

(tab.3): MQ, NQ, HQ and discharge quotient NQ/HQ of Pleier and Roach Springs from 2005 to 2006 and 2008 to 2009, calculated from day mean values. Data from measurement campaigns 2005 and 2006 have been provided by Joanneum Research

	Pleier		Roach	
NQ (l/s)	11,16	6,9	19,68	21,33
HQ (l/s)	43,95	21,37	529,1	403,32
MQ (l/s)	19,48	12,48	91,04	103,61
NQ/HQ (l/s)	0,25	0,32	0,04	0,05
	june05-july06	june08-july09	june05-july06	june08-july09

It is obvious that the database of Pleier Spring for the years 2008/2009 shows a systematic difference in discharge of about 50% to the years 2005/2006. This is probably due to an error in data acquisition or data processing, or because of the fact that not all springs of the northern plateau where included in spring logging in 2008/2009. Since the discharge quotients of both years are of similar magnitude, which indicates an equal dynamic for both databases, it is still possible to analyse the data.

The NQ value of Roach is 21.33 litres, which is the minimum volume available for discharge in the year 2008/2009, while Pleier has a minimum volume of 6.9 litres. The differences in HQ values of 2005/2006 to the year 2008/2009 is a result of the intense snowfalls in winter 2005/2006 and snowmelt in spring 2006.

Derived from their hydrographs, discharge coefficients of the Pleier and Roach Springs have been calculated for the time from spring to fall 2009. The hydrograph of the measuring point Pleier shows three different coefficients of discharge (fig.33), α1 (0.011-0.014), α2 (0.002-0.006) and α3 (0.003-0.004, see also table 4), which appear frequently within the hydrograph (fig.34). Roach Spring shows two iterative discharge coefficients (fig.34 and fig.36), α1 (0.078-0.081) and α2 (0.020-0.035, see also table 5).

The transition from α1 to α2 of Pleier Spring takes place at about 16 (l/s) and from α2 to α3 at roughly 13 (l/s) (fig.35 and tab.4). Transition from α1 to α2 of Roach Spring is at a discharge rate of approximately 160 (l/s) (fig.36 and tab.5).

(tab.4): average discharge coefficients of the Pleier Spring, with their respective initial (Q0 [l/s]) and final (Qt [l/s]) discharge volumes of each base runoff recession curve (fig.32)

Pleier	t0	Q0 [l/s]	t	Qt [l/s]	Δt [d]	α [1/d]
α1	07.04.2009	20.62	27.04.2009	15,63	20	0,0125
α2	28.04.2009	15.73	19.06.2009	11,68	52	0,004
α3	27.06.2009	12.93	03.09.2009	11,15	36	0,0035

(tab.5): average discharge coefficients of the Roach Spring, with their respective initial (Q0 [l/s]) and final (Qt [l/s]) discharge volumes of each base runoff recession curve (fig.33)

Roach	t0	Q0 [l/s]	t	Qt [l/s]	Δt [d]	α [1/d]
α1	11.03.2009	317,4	18.03.2009	166,38	8	0,0795
α2	20.03.2009	163,64	29.03.2009	133,89	10	0,0275

Discharge coefficients α2 and α3 from the hydrograph of Pleier Spring represent a low discharge over a long period of time. They do not differ very much in magnitude. Generally speaking, low volume discharge is a predominant feature of Pleier Spring compared to Roach. Only α1 recession straight line shows a steeper inclination within the hydrograph, which stands for a relatively bigger discharge (fig.33 and tab.4).

The high value coefficient α1 of Roach Spring depicts fast discharge of big volumes within a relatively short time. Low value α2 shows a slower flow out of discharge with smaller volumes per time (fig.34 and tab.5).

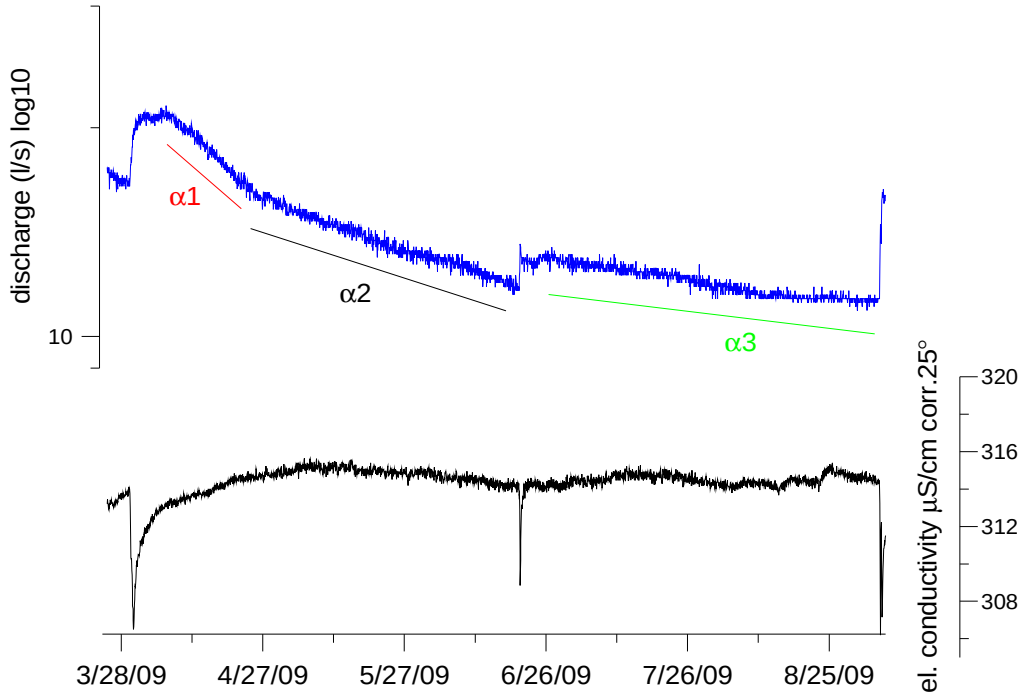

(fig.33): extracted semilog graph from Pleier Spring hydrograph and electric conductivity graph for the recession period from tab. showing discharge coefficients α1, α2 and α3

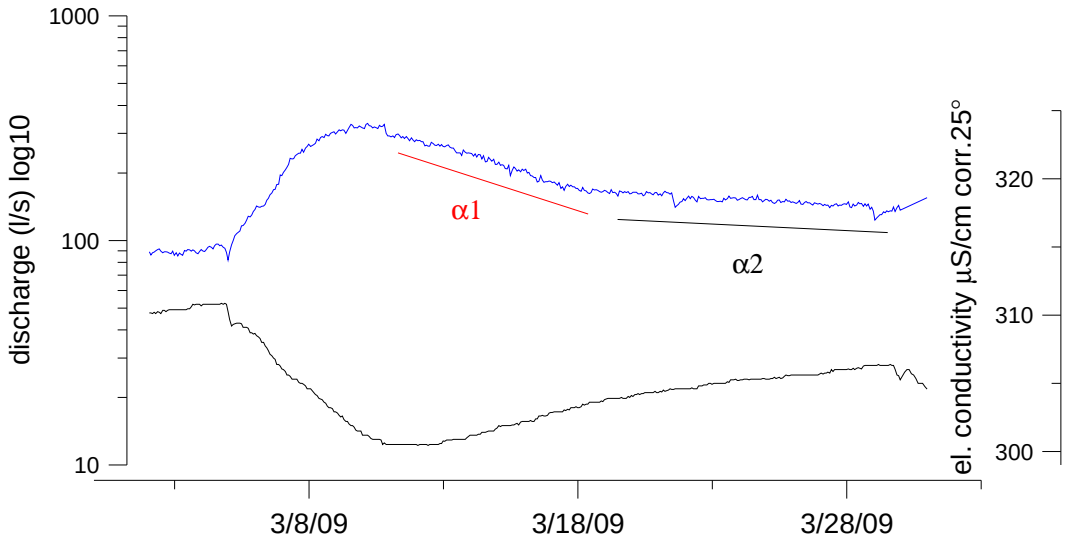

(fig.34): extracted semilog graph from Roach Spring hydrograph and electric conductivity graph for the recession period from tab. showing discharge coefficients α1, α2

Figures 35 and 36 show the hydrographs of Pleier and Roach Springs for the time from April 2008 to October 2009, as well as the respective curves for electric conductivity and temperature, graphs are based on day mean values.

Precipitation is displayed as a bar plot in figures 35 and 36. Due to data shifts of the ombrograph, a maximum accuracy of one day can be given for the rainfall recordings.

Maximum discharge rates of both springs are reached during December and in the time from March to April, the first because of snowmelt during a mild winter period, the latter because of snowmelt in spring. Minimum discharge flows out during the summer (fig.35 and fig. 36).

Although both springs have very different magnitudes of discharge, they show similar electric conductivity and temperature values (fig.35, fig.36 and tab.2), since both drain the same hydrogeologic area Turiawald, and are affected by similar lithologies and geologic structures (fig.7, fig.8 and fig.9).

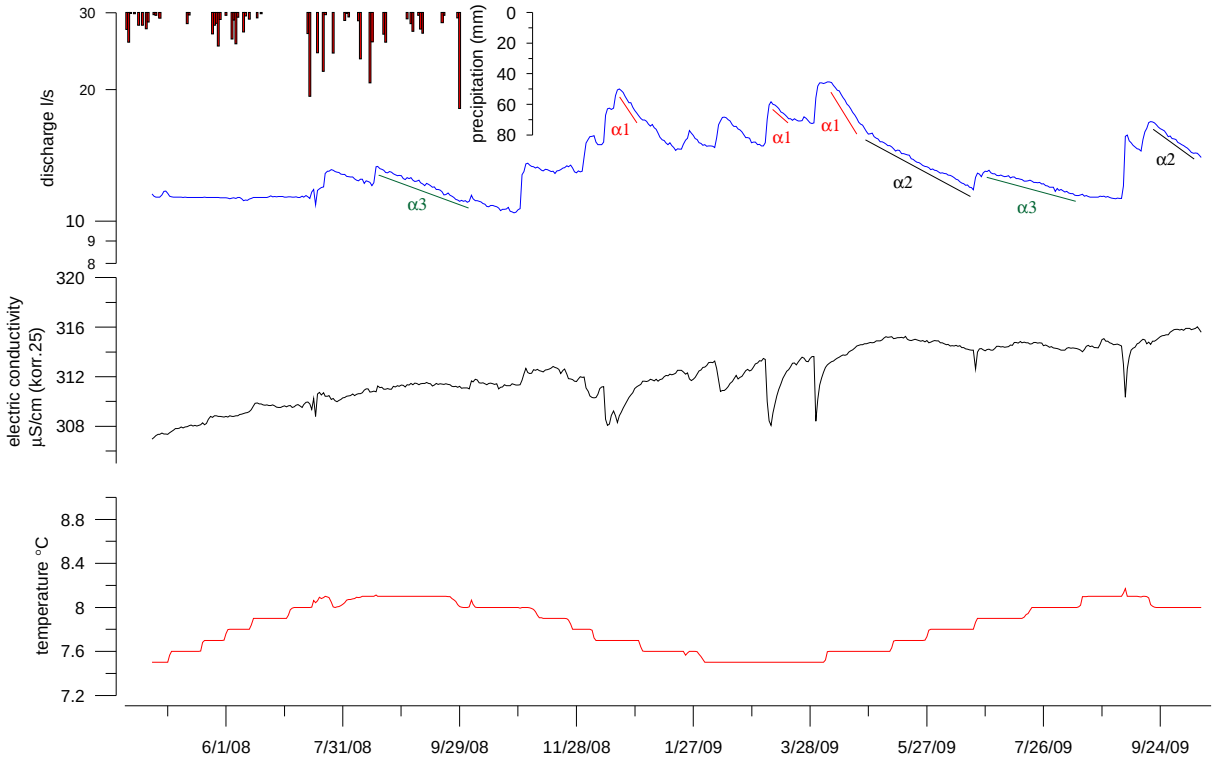

(fig.35): hydrograph of the Pleier Spring (blue), with its respective electric conductivity (black) and temperature (red) graphs, precipitation from April to September 2008 is displayed by the bar plot, α values and their respective straight lines

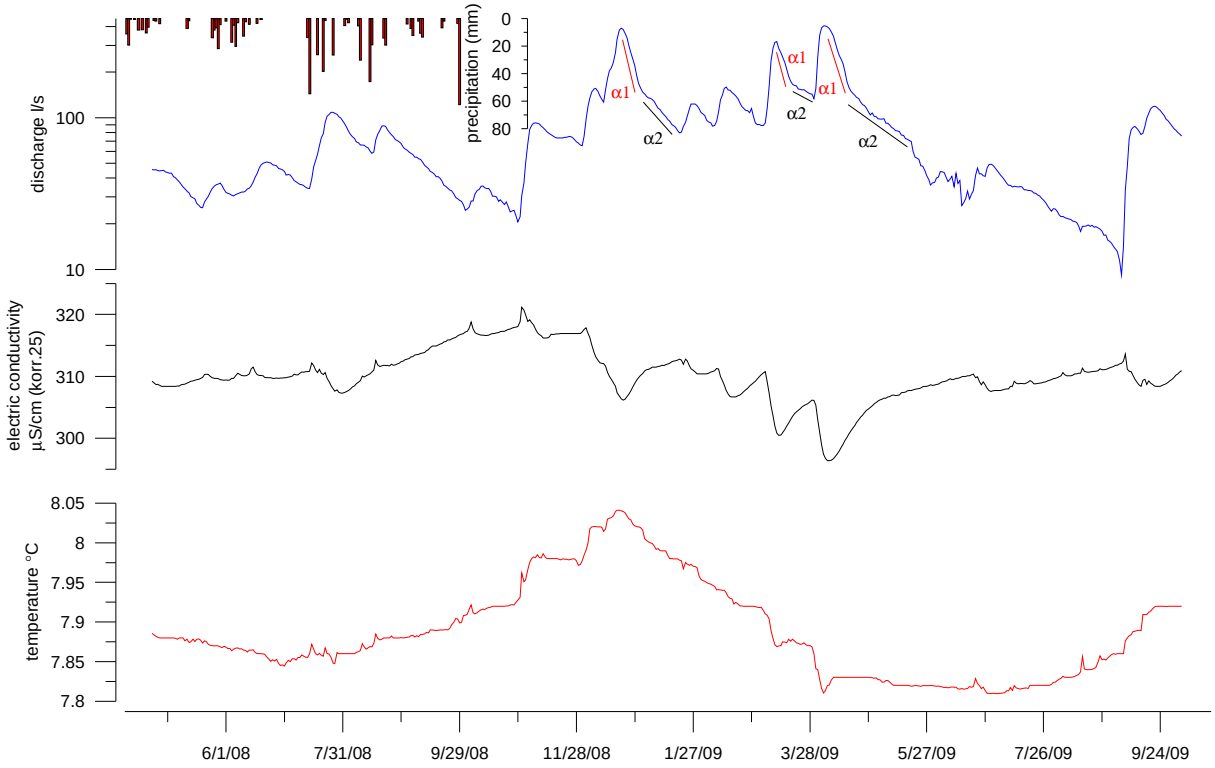

(fig.36): hydrograph of the Roach Spring (blue), with its respective electric conductivity (black) and temperature (red) graphs, precipitation from April to September 2008 is displayed by the bar plot, α values and their respective straight lines

Electric conductivity of both springs is inversely proportional to the discharge: higher flow rates are followed by a decrease in conductivity. If discharge increases after a longer period of recession, the conductivity of Roach Spring often rises up before sharply decreasing (fig.36), while Pleier shows almost no reaction of this kind (fig. 35). Four days after a severe increase of discharge, the hydrograph of Roach Spring shows a maximum decrease of electric conductivity. Pleier Spring reacts much faster and the time lag between maximum rise of discharge and maximum decrease of electric conductivity is only fifteen hours (fig.37).

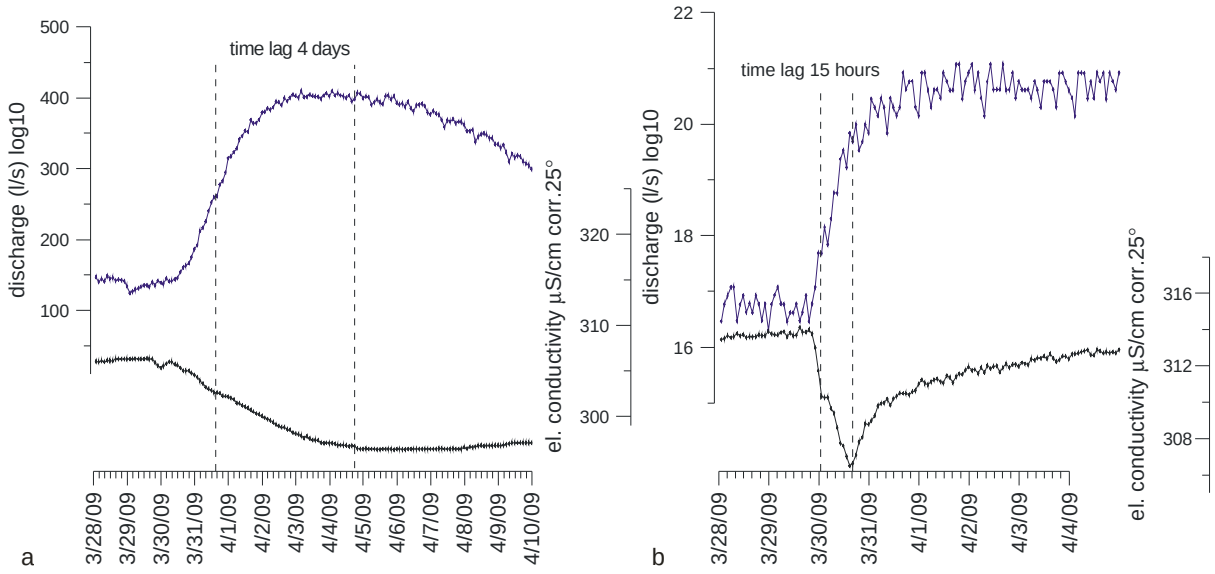

(fig.37): time lags between strongest increase of discharge and maximum decrease of electric conductivity, a) Roach Spring, b) Pleier Spring

Changes in temperature due to discharge variation are marginal at Roach and almost not observable at Pleier. Single strong precipitation events cause an increase of the flow rate at Roach Spring within a single day, while Pleier shows a lower hydraulic reaction to a recharge input pulse, with a time lag of one to three days between an increase of discharge and the precipitation event (fig.35 and fig.36).

4.3.4 Resources of Water

As discussed in chapter 4.3.2, data gained from spring logging was calculated to establish recession straight lines and α values. For further analysis and interpretation of the hydrographs falling limb, the theoretical total volume of groundwater at the start of recession was calculated. This total volume has been interpolated from the recession straight lines and their corresponding α values (figs. 33, 34 and tabs. 4, 5), which are linked to single unique discharge regimes and volumes.

Hydrographs of both of the investigated springs show two iterative linked recession straight lines along their run with the respective inclination values α1 and α2. Pleier Spring also features a third recession value, α3 (fig.35 and fig.36). By applying the equations mentioned in chapter 2.4.3, it is possible to calculate not only the theoretical total volume, but also the single volumes for each discharge micro regime linked to an α value.

At Roach Spring, the event water volume V1 of 138.03 million litres (fig.38 and tab.6) runs off at the beginning of the recession, followed by the base flow volume V2 with 812.16 million litres (fig.38 and tab.6). A total volume V0 of 950,19 million litres (tab.6) can theoretically be discharged from the beginning of the recession to the end of the hydrograph, under the assumption that α values remain constant.

The values to calculate these volumes have been selected from the period of 11.03.2009 to 29.03.2009 (see tab.5). At these dates of the hydrograph of Roach Spring, both α1 and α2 can be identified clearly and the end of the recession is clearly marked by a rising limb.

(tab.6): initial discharge rates Q01 and Q02 and the corresponding volumes of water V1 and V2 (fig.38) of Roach Spring, V0 is the total initial volume of water at the beginning of discharge

Q01 (l/s)	317,4	V1 (l)	138,03 * 10^6
Q02 (l/s)	188	V2 (l)	812,16 * 10^6
		V0 (l)	950,19 * 10^6

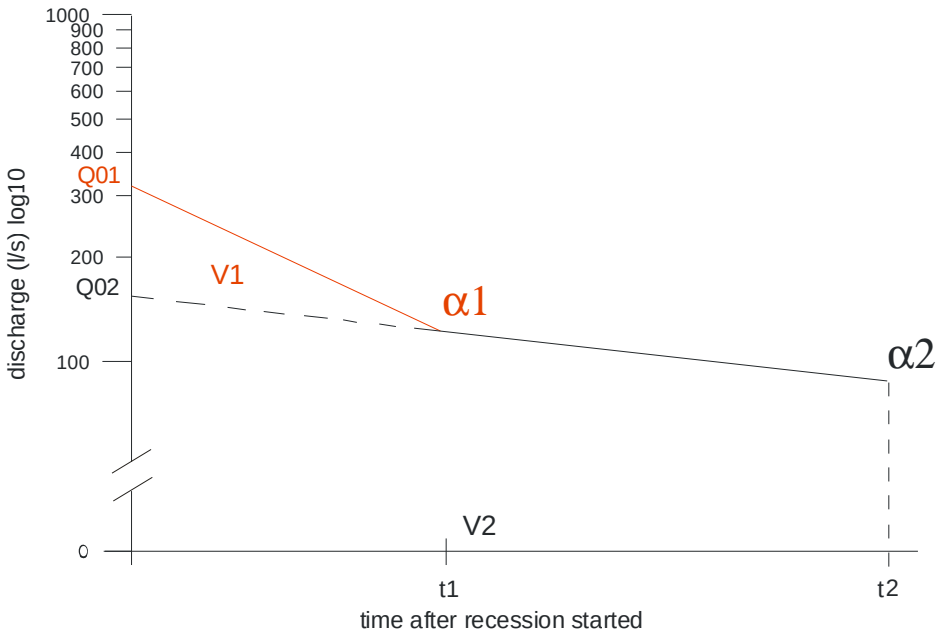

(fig.38): recession straight lines of Roach Spring from (fig.34), with the two micro regimes of discharge and corresponding volumes V1 and V2 (tab.6), Q01 marks start of recession, t1 and t2 correspond to Δt (tab.5)

Pleier Spring shows one relatively fast draining discharge volume V1 (fig.39, tab.7) with 21.72 million litres, and the intermediate V2 (fig.39, tab.7) featuring a volume of 44.64 million litres which can flow out. The base flow is V3 (fig.39, tab.7) with 302,4 million litres, the total available volume V0 (tab.7) is 368,7 million litres.

The values to calculate these volumes have been selected from the period of 07.04.2009 to 03.09.2009 (see tab.4). At these dates of the hydrograph of Pleier Spring, α1, α2 and α3 appear consecutively. Between the final discharge of α2 straight line and initial discharge α3, a disturbance is visible on the hydrograph (fig.33). To perform a consistent calculation, the recession straight lines in figure 39 have been composed by parallel adjustment of the α3 line.

(tab.7): initial discharge rates Q01,Q02 and Q03 and the corresponding volumes of water V1,V2 and V3 (fig.39) of Pleier Spring, V0 is the total initial volume of water at the beginning of discharge

Q01	20,62	V1 (l)	21,72 * 10^6
Q02	17,1	V2 (l)	44,64 * 10^6
Q03	14	V3 (l)	302,4 * 10^6
		V0 (l)	368,7 * 10^6

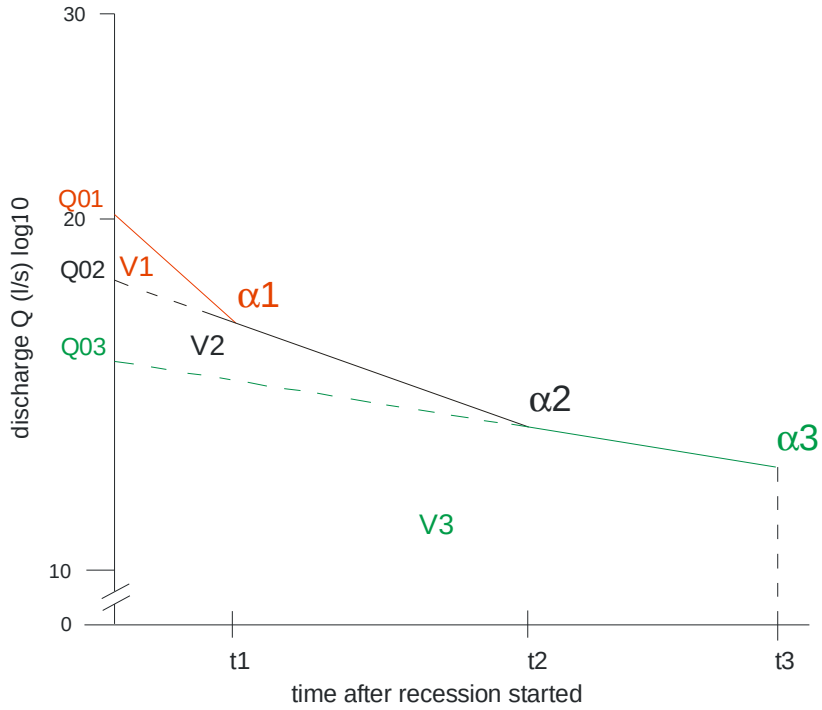

(fig.39): recession straight lines of Pleier Spring from (fig.32), with the two micro regimes of discharge and corresponding volumes V1, V2 and V3 (tab.7), Q01 marks start of recession, t1, t2 and t3 correspond to Δt (tab.4)

It is observable that Roach spring has many more resources for the discharge of water in both event influenced and base flow volumes. Both springs discharge the largest volumes from their base flow volumes V2 (Roach) and V3 (Pleier). The base flow of Roach Spring is about two times bigger than the base flow of Pleier. The total theoretical discharge V0 at Roach is three times higher. The relation of base flow to event water volumes is roughly 6:1 at Roach Spring, while at Pleier Spring this relation is 4.5:1, if V1 and V2 are considered as event water.

5. Discussion and Interpretation

5.1 Structural Geology and Morphology

5.1.1 Turiawald Plateau

The altitude of the plateau is descending from the south east to the north west (fig.25). The formations of crystalline rocks, i.e. marbles and diaphtorites in the south and south east of Turiawald (fig.8), are known to be in contact with the Sattnitz Conglomerate. Thrust planes and slickensides of St. Ruperti outcrop have an average dip direction to the north west (fig.17).

Since the north western part of Turiawald conglomerates is underlain by fine grained clastic formations and the south eastern part by subjacent crystalline rocks (fig.8), it can be assumed that the plateau bears on the uplifted competent crystalline rocks in the southeast, while moving downwards on the incompetent layers of fine clastic rocks in the northwest. The fine grained clastic formations are squeezed out in a westerly direction by the pressure of the overlying conglomerates. The resulting mass deficit of the subjacent clastics caused the brittle conglomerate layer to bow and finally break.

The break occurs mainly along pre-existing discontinuities, which is indicated by the correlation of strike directions of joints, sinkholes and lineaments of Turiawald with striking of joint sets of the basement rocks and regional lineaments (fig.21 and fig.24).
In addition the mass movement also creeps down the western slope, therefore it is assumed that below the western part of Turiawald, friction between the moving fine clastic rocks and the constraining conglomerate induces horizontal normal tensile stress upon the brittle top layer. This leads to the formation of joints and fractures with both orthogonal and perpendicular directions to the border of the conglomerate layer (fig.25 and fig.26).

A NW/SE striking single joint opening is located at the south eastern part of the plateau, which shows an aperture of one metreand a length of approximately 40 metres. Along the lengthening of this crack also several sinkholes can be found aligned in a row, following the strike of the joint. This indicates a tectonic origin of the sinkholes. No signs could be found to verify the assumption, that these sinkholes are formed by karst formation, as suggested by other authors.
The large numbers of sinkholes, depressions and joint openings appearing on the Turiawald plateau, also in a respective distance from the escarpments, and the general undulous

morphology of the plateau, indicate a progressive, backwards directed advance of the slope tectonics, which causes the platform to break up. This occurs not only in the border areas of the plateau and its centre, but also towards the most elevated south eastern area (fig.25).

The springs in the north and west of Turiawald indicate the presence of water at the contact area between conglomerate and basement rocks. The water pressure reduces friction and supports the movements of conglomerate blocks above the subjacent layers, resulting in an increase of joint and fissure openings.

5.1.2 Mass Movement of the Western Slope

During Wuerm Glacial Period, Turiawald plateau was covered by several hundred metres of ice from the Drau Glacier, which was flowing from west to east (Fellner 1993). The ice also supported the western flank of the plateau. When the glacier retreated, the counter bearing of the ice was removed and the over steepened western flanks of Turiawald started to move.

Blocks are separated from the in situ conglomerate of the plateau by joint planes, which were pre-existing or caused by breakup of the conglomerate layer. Conglomerate blocks and slabs that are fully separated from the platform by joint planes and have at least one vertical joint plane, which daylights to the west, are suspected to move downhill.

The type of mass movement in this area can be classified as a complex mass movement (after Hutchinson 1988), for the following reasons:

At least three different types of slope failure at the rock faces of Turiawald could be identified (fig.19d and fig.29):

- rock toppling failure, which is especially predominant in the northern area of the western slope
- rock slumping failure, which is occurring only in a few cases
- translational movement of blocks, also only observed in small numbers

Blocks and big mass movement bodies situated at a minimum distance of 500 m from the rock faces also show these types of movement.

Because of the fact that these different mechanisms of movement appear together, it is assumed that no single sliding plane is present within the mass movement body, which

consists of conglomerate blocks and debris as well as fine clastic rocks. There are also no incidents of recent rapid movement known at the western slope itself, but several indicators for slow movement have been observed:

-undulatory topography
-bow shaped growth of trees
-roof fall incidents affecting the coal mine “Augstistollen”
-convex slope form

Considering these aspects, the mass movement can also be described as creeping (after Glawe & Moser, 1989 and Hutchinson, 1988).

At two locations at the foot of the western rock faces, blocky debris from past rock falls can be found. It is assumed that this debris broke off during the initial stage of a slab or block being removed from the in situ rock mass, representing its crown or upper part.

Since fine clastic rocks formations and coal beds found inside the mass movement have the same structural orientation as their respective linked block, it is stated that these formations are brought up to daylight by the rotation of the blocks.
Since there are no fine clastic rocks or coal occurrences at the surface of the southern part of the western slope, it may be stated that in this area the rotational movement of blocks is less intense as in the north, which is also indicated by the structural data (fig.29).

5.2 Hydrogeology

5.2.1 Aquiclude Morphology

At the northern part of the western slope, the basal clastics of the Penken Formation are moving downhill attached to their respective blocks. Thus, they are affected by rotation of blocks, which makes the fine clastic rocks layer discontinuous and diffuse in this area. An uneven profile of the aquiclude containing both morphologic heights and depressions has to be assumed. Outcrops of fine grained clastics may be the high points of such a structure. Because of this, the position of the aquiclude cannot be determined more exactly and has to be considered variable (fig.31).
There are no occurrences of fine clastic rocks, coal or wetlands at the surface of the southern part of the western slope. As explained before, translational movement of blocks in this area is predominant, which is also indicated by structural data (fig.29). This type of downward movement of blocks also displaces the underlying fine clastic rocks, but do not crop out, indicating that the basal neogene clastics layer is continuous in this area.

Because of the fact that the thrust planes of the marbles of St.Ruperti are dipping to the northwest (fig.17), it may be assumed that the whole south eastern part of Turiawald is underlain by crystalline rocks, which was also assumed by preliminary studies (Poltnig et al. 2007, Griem et a. 1992, fig.7 and fig.8). It is suggested that these crystalline rocks also act as an aquiclude bed in this area.
Crystalline and fine grained clastic parts of the aquiclude seem to dip towards the north west. The water from the western part of the catchment area also runs in this direction, which is illustrated by the fact that all springs featuring high discharge rates are on the northern and western flanks of the plateau. The NE/SW striking, valley shaped lineament in which Roach Spring is situated (fig.31) can probably act as a draining element and direct the groundwater westward from the mass movement area to the deepest point of the slope where Roach Spring is located.

5.2.2 Hydrograph Analysis and Natural Tracers

Roach shows features of a karst spring, including a low quotient of discharge NQ/HQ of 0.05 and strongly varying minimum NQ and maximum HQ discharge, as well as relatively high α values of an order bigger than 10^{-2} for both base flow and event water (tab.8 and tab.9). Since no clear signs of karstification were found on Turiawald or its foreland, it is assumed that these characteristics are caused by open, well connected joints and fissures on the plateau and voids provided by the mass movement body.

Hydraulic reaction due to precipitation events appears within one day or less and the transit time of water moving through the aquifer conduits is approximately four days, shown by time lag analysis (electric conductivity decreases during an increase of discharge).

(tab.8): MQ, NQ, HQ and discharge quotient NQ/HQ of Pleier and Roach Springs from 2008 to 2009, calculated from day mean values.

	june08-july09	june08-july09
	Pleier	Roach
NQ (l/s)	6,9	21,33
HQ (l/s)	21,37	403,32
MQ (l/s)	12,48	103,61
NQ/HQ (l/s)	0,32	0,05

(tab.9): average discharge coefficients of the Pleier and Roach Springs

Pleier	α [1/d]	Roach	α [1/d]
α1	0,0125	α1	0,0795
α2	0,004	α2	0,0275
α3	0,0035		

Pleier Spring has a quotient of discharge of 0.32 and does not show strong variations in minimum and maximum discharge, which is characteristic for a more retentive storage milieu (tab.8). Pleier Spring only has one single value, α1, which shows an order of 10^{-2} and represents a relatively fast flow out. The coefficients α2 and α3, which drain the bigger volumes, indicate by their magnitude of 10^{-3} (tab.9) discharge from aquifers of smaller voids like narrow joints and aquifer matrix.

Hydraulic reaction to precipitation can take place within one to three days. The transit time indicated by a decrease of electric conductivity is only fifteen hours.

Roach Spring often shows for a short period an increase of electric conductivity at the beginning of a rising limb on the hydrograph (fig.36). It is assumed that a part of the water remains in a storage regime where it interacts strongly with the carbonate conglomerate and

water bound CO2, providing a higher mineralization. Such a regime could be provided by the mass movement body and the big surface of the conglomerate debris. This mass movement water is then flushed out first by an increasing hydraulic gradient.
The electric conductivity graph of Pleier Spring shows almost only a decrease due to changes of discharge (fig.35). Therefore it is assumed, that infiltrating water moves into an aquifer where, due to a smaller surface of the aquifer rock or the absence of CO2, no such reactions take place and the spring is only slightly influenced by a debris body.

There is an inconsistence between discharge coefficients, discharge quotients, and the time lags of water transit and hydraulic reaction.
The α values and NQ/HQ quotient of Roach Spring show characteristics of a fast draining spring, and only a short time passes between precipitation and a hydraulic reaction. However, the transit time of the water through the aquifer conduits is several days.
The fast hydraulic reaction and the high maximum discharge can be explained by rapid infiltration of precipitation water into the mass movement body, illustrated by α1 which is linked to the theoretical discharge volume V1 and resembles 14% of total discharge from Roach.
Groundwater flowing from the plateau to Roach Spring passes through the mass movement, where water from the less permeable plateau storage mixes with highly mineralized water from the much more permeable mass movement storage, resulting in the smaller coefficient α2. It is assumed that this process takes several days. This assumption can explain the time lag between maximum discharge increase and electric conductivity decrease.

Pleier Spring is mainly characterized by α2 and α3 values of similar magnitude indicating slower discharge, but also α1 with a magnitude typical for fast discharge. The latter indicates fast transport of water through large voids like joint openings, which is supported by the presence of lineaments on the northern plateau. V1 is the linked theoretical discharge volume of α1 and represents 5% of the total discharge of Pleier.
The volume V1, represented by the discharge coefficient α1, is also held responsible for the fast dilution causing the decrease of electric conductivity, while α3 illustrates slow discharge from narrow joints or a matrix aquifer. Coefficient α2 is assumed to be an intermediate value between α1 and α3.

The additional hydrograph analysis results prove that Roach Spring drains approximately 80% of the Turiawald catchment, fitting quite well with the existing assumption of about 75% (Winkler et al 2008, Poltnig et al. 2007). Roach Spring discharges at 103.6 (l/s) about 82% of the total average annual discharge (116,1 l/s, which is the sum of MQ values of Roach and

Pleier Springs, plus the anticipated 10 (l/s) from Hojoutz water gallery) measured in 2008/2009. Pleier Spring drains approximately 13% of the total catchment. The annual average discharge of 12.48 (l/s) represents 11% of the total discharge of Turiawald.

The relatively high discharge of Roach Spring compared to its recharge area can be explained by the inclination of the aquiclude, which is gently dipping from south east to north west, thus the groundwater flows generally in this direction.

6. Conclusion

6.1. Failure Mechanism and Kinematics

The conglomerate platform Turiawald is broken up and shows a step-like downward morphology from the south east to the north west (fig.40). The southerly subjacent crystalline basement lifts up the most south eastern conglomerate slab bearing on it, while the rest of the platform moves downhill in a north western direction. The thrust planes of the crystalline basement dipping to the north west are assumed to form a gliding plane for the hanging conglomerates in the south east, while below the north western parts of Turiawald incompetent fine clastic rocks enable gliding of the hangingwall.
The expansive downward movement of conglomerate slabs and blocks results in an undulous morphology of the plateau, which consist of depressions and elevations. These appear to be similar to horst and graben structures.

The break up of the plateau is also illustrated by its lineaments, joints and sinkholes. These have main strike directions correlating to the strike of joints sets of basement rocks and regional lineaments. The latter are linked as Riedel shear planes to the Periadriatic Line. Thus, it is assumed that the joint sets and lineaments of Turiawald are mostly formed along pre-existing discontinuities.

The most sinkholes, joint openings and joint sets can be found in the west of the Turiawald Plateau and at the foot of its western rock faces, often featuring orientations of strike directions parallel and perpendicular to the escarpments.
At the western flank of the Turiawald plateau, the incompetent footwall of fine clastic rocks of the Penken Formation, evades the pressure from the overlying Sattnitz Conglomerate and are squeezed out into the western foreland. As a consequence of this movement, and the resulting mass deficit, the competent hangingwall conglomerate starts to sink down and breaks up into distinct blocks. These continue to move further downhill and break up due to the movement. Together with conglomerate debris and fine clastic material, these blocks form the mass movement body of the western slope.

The blocks of the western slope show the following movement types:

- rock toppling failure
- rock slumping failure
- translational movement of blocks

As a résumé, the whole mechanism of deformation of western Turiawald Plateau and the consequent mass movement of its western foreland can be described as a “hard on soft” system (after Poisel and Eppensteiner 1989).

Because of the simultaneous appearance of block failure modes, it is assumed that no single failure plane is present and no fast displacement takes place. This suggests that creeping is the type of movement of the mass movement body below the western rock faces (after Glawe, Moser, 1989). This type of mass movement is due to the fact that several modes of failure appear together and are classified as a complex mass movement (after Hutchinson 1988).

An imminent danger of being affected by the mass movement of Turiawald or a consequent rock fall can be excluded for the villages Roach and Penken. The minimum distance between the rock faces and buildings is roughly 2 kilometres, but rock fall debris was only found directly at the toe of the faces of the western escarpment. Dense woods and soft underground would provide proper damping space for such an incident. There have been no signs found indicating significant recent rapid failure or movement of blocks at the faces, and no signs of fast movement have been observed at the mass movement body.

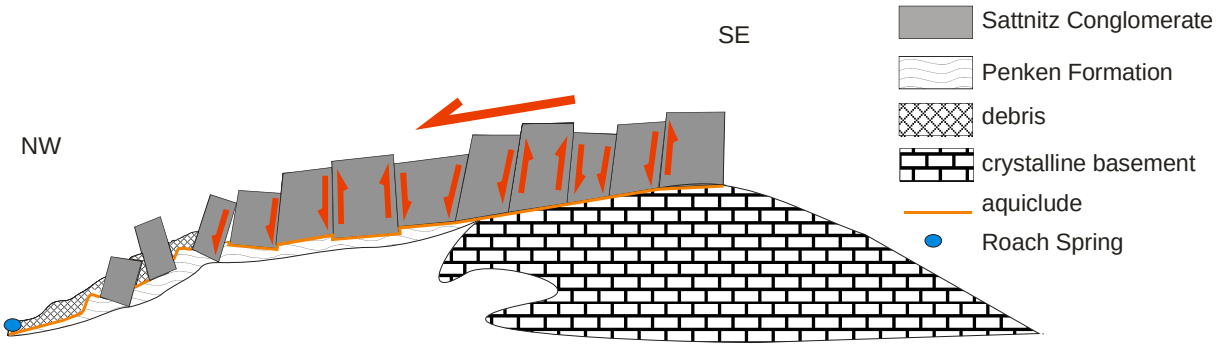

(fig.40): sketch map of Turiawald, moving downwards to NW, thickness of crystalline basement is unknown

6.2 Hydrogeology

Both investigated springs are bound to the lithologic contact of the permeable Sattnitz Conglomerate and the impermeable and neogene fine clastic rocks of Penken Formation.
The two springs show distinct features in their discharge behaviour, which are bound to geologic and morphologic features of their respective recharge areas. Joint openings and sinkholes at the surface of the plateau are assumed to enforce infiltration of precipitation and therefore prohibit surface runoff.

While Pleier Spring is situated close to the northern escarpments at an altitude of 650m, Roach is located at the base of the mass movement area at an altitude of 550 metres (fig.40), which is about one kilometre from the plateau margins.
Considering discharge quotients and coefficients, Pleier is draining an aquifer situated within the plateau, which mainly consists of narrow joints or aquifer matrix. Only a small part of the discharge is related to fast infiltration of precipitation due to joint openings.

Roach shows clear characteristics of a karst spring, although these are also related to the joint openings of the broken platform of Turiawald as well as the resulting mass movement.
As opposed to Pleier Spring, Roach is strongly influenced by the mass movement. On the one hand it allows rapid infiltration of precipitation due to the large voids of the conglomerate debris, on the other hand it buffers water flowing out of the plateau.

The mass movement also influences the position and morphology of the aquiclude on the western slope. The aquiclude consists of crystalline rocks of the prepermian basement rocks in the south eastern part of Turiawald, and neogene fine clastic rocks in the west and north west. It is gently dipping towards the north west, where the strongest discharging spring, Roach Spring, is located (fig.40).
Within the mass movement area, the fine clastic layer has been displaced and discontinued by the downward creep of the slope, and rotational movements of conglomerate blocks formed a molded surface of the aquiclude in the north of the western slope (fig.40). In the south, the aquiclude has been moved downwards but still seems to be continuous.

Altogether, the mass movement influences the hydrogeologic system of Turiawald in two ways: First, the western part of the aquiclude is deformed and displaced downhill, especially in the northern area of the western slope. Second, the mass movement body is added as an additional, very quickly discharging groundwater storage to the aquifer system of the plateau.

7.Literature

Bauer, F. K., Cerny, 1., Exner, C., Holzer, H.-L., v. Husen, D., Loeschkc, J., Suette, G. & Tessensohn, F. 1983. Erläuterungen zur geologischen Karte der Karawanken 1:25,000, Ostteil. Geol. Bundesanstalt, Wien.

Bögel, H. 1975. Zur Literatur über die "Periadriatische Naht“. Verh. geol. Bundesanstalt 1975, 163-199.

Boyer, S.E., Elliott, D., 1982. Thrust systems. American Association of Petroleum Geologists Bulletin 66, 1196–1230

Brosch, F.J. & Kurz, W.: Fault damage zones dominated by high-angle fractures within layer-parallel brittle shear zones: examples from the Eastern Alps.- Geol. Soc. Spec. Publ., 299, 75-95, 2008.

Bundesamt für Eich– und Vermessungswesen 2005 Österreichische Karte 1:50.000 (ÖK 50)

Claasen et al., Die Permotrias und ihr Grundgebirge zwischen Faaker See und Turiawald südöstlich von Villach (Kärnten/Österreich), Jb.Geol. B.A., S 391-413

Eisbacher G. H., (1996): Einführung in die Tektonik. 374 S., Ferdinand Enke Verlag, Stuttgart, 1996.

Fellner, D., 1993 , Die Massenbewegungen der Sattnitz (Kärnten, Österreich), Jb.Geol. B.A., S 315-325

Glawe U. & Moser M., (1993): Meßtechnische und theoretische Bearbeitung von Bergzerreißungen und Blockbewegungen. Felsbau 11 (1993) Nr. 5, pp.235-250.

Gosen, W., von 1989. Fabric development and the evolution of the Periadriatic Lineament in southeast Austria. Geol. Mag. 126, 55-71.

Griem et al., 1992, Sedimentologie und Sedimentpetrographie des tertiären Sattnitzkonglomerats zwischen Villach und Klagenfurt (Kärnten, Österreich), Jb.Geol. B.A., S 27-36

Hancock, P. L., 1985, Brittle microtectonics: principles and practice, Journal of Strucural Geology, Vol.7, pp. 437 to 457

Hölting B., & Coldewey W. G., (2005): Hydrogeologie, 6. edition (2005), Ferdinand Enke Verlag, Stuttgart, 348 S.

Hutchinson, J.N. (1988): General report: Morphological and geotechnical parameters of landslides in relation to geology and hydrogeology. – In: BONNARD, C. (Ed.): Proc., Fifth International Symposium on Landslides, A.A. Balkema, Rotterdam, Vol.1, 3-35.

KaGis Kaernten, Amt der Kärntner Landesregierung Abt.20 / Landesplanung, DHM 10m der triangulierungs Blattschnitte

Kahler, E, 1953. Der Bau der Karawanken und des Klagenfurter Beckens. Carinthia II, pp. 5-78.

Klaus, W., 1956. Mikrosporenhorizonte in Stid- und Ostkarnten. Verhandlungen der Geologische Bundesanstalt, Wien, pp. 250-255.

Kresic N., (2007): Aquifers and Aquitards, S.224-245, Hydrogeology and Groundwater Modelling,
807 S.; Boca, Raton, Florida, 2007

Langguth H.R., Voigt R., 2004, Hydrogeologische Methoden, Springer, Berlin, pp. 203

Laubscher, H. P. 1970. Das Alpen-Dinaridenproblcm und die Palinspastik der südlichen Tethys. Geol. Rdsch. 60, 813-833.

Laubscher H. P. 1983. The late Alpine (Periadriatic) intrusions and the lnsubric Linc. Mere. Soc. geol. Italia 26, 21-311.

Laubscher, H. P. 1988. Material balance in Alpinc Orogeny. Bull. geol. Soc. Am. 100, 1313-1328.

Madritsch H & Millen B. M. J., (2007): Hydrogeologic evidence for a continuous basal shear zone within a deep-seated gravitational slope deformation (Eastern Alps, Tyrol, Austria). Landslides 4 (2007), 149-162.

Maillet E., (1905): Essais d´hydraulique souterraine et fluviale, 218 S.; Paris, 1905.

Meschede M. 1994, Methoden der Strukturgeologie, Enke, Stuttgart, 112 pp.

Nemes et al., 1997, The Klagenfurt Basin in the Eastern Alps: an intra-orogenic decoupled flexural basin, Tectonophysics, P 189-203

Nemcok, A, (1977): Geological/Tectonical Structures – an essential condition for Genesis and Evolution of Slope Movements. Bull. Int. Assoc. of Engineering Geology, Vol.16, 127-130, Krefeld

Papp, A., 1951. Ober die Altersstellung der Terti/irschichten von Liescha bei Priivali und Lobnig. Carinthia II 141, 62-64.

Passchier, C.W. & Trouw, R.A.J. (2005): Microtectonics 2nd edition. Springer, Berlin Heidelberg.

Poisel et al., 1988, Gang und Gehwerk einer Massenbewegung Teil1, Geomechanik des Systems „Hart auf Weich“, Felsbau 6, S189-194

Poisel et al., 1989, Gang und Gehwerk einer Massenbewegung Teil2, Massenbewegungen am Rand des Systems „Hart auf Weich“, Felsbau 7, S 16-20

Polinksi, R.K., Eisbacher G.H., 1992, Deformation during polyphase oblique convergence in the Karawanken Mountains, southeastern Alps, Journal of structural geology, Vol. 14, pp1203 to 1213

Poltnig et al., 2007, Hydrogeologie Sattnitzberge-Sattnitzplateau-West KA42/04, unveröff. Ber., Inst. f. Wasser Ressourcen Management, S 110

Sauter, M., 1992, Quantification and Forecasting of Regional Groundwater Flow and Transport in a Karst Aquifer, (Gallusquelle, Malm, SW. Germany), TGA, C13, 150 pp.

Schmid, S. M., Aebli, H. R., Heller, F. & Zingg, A. 1989, The role of the Periadriatic Line in the tectonic evolution of the Alps. In: Alpine Tectonics (edited by Coward, M. P., Dietrich, D. & Park, R. G.). Spec. Pap. geol. Soc. Am. 45, 153-171.

Schönlaub, H. P. 1979. Das Paläiozoikum in Osterreich. Abh. geol. Bundesanstalt 33, 124S.

Tollmann, A., 1985. Geologie von Osterreich (Zentralalpiner Teil), 2. Deuticke, Wien, 680 pp.

Winkler, G**.**, Poltnig, W. & J. Schlamberger (2008): Hangtektonische und tektonische Beeinflussung des Grundwassersystems Sattnitz,.- Computeranwendungen in Hydrologie, Hydrogeologie und Geologie, Beiträge zur COG-Tagung Salzburg 2007, Wichmann, Heidelberg: 38-46

Wyllie, D.C. & Mah, C.W. (2004): Rock Slope Engineering: Civil and Mining. 4th ed, SponPress, London.

Appendix A

1. Ombrograph data

date	mm of rainfall		date	mm of rainfall
april				
11.04.2008	112		july	
12.04.2008	195		13.07.2008	138
13.04.2008	6		14.07.2008	546
15.04.2008	8		18.07.2008	263
17.04.2008	84		21.07.2008	384
19.04.2008	83		22.07.2008	16
21.04.2008	106		26.07.2008	265
22.04.2008	63		01.08.2008	52
25.04.2008	16		02.08.2008	6
26.04.2008	20		03.08.2008	30
28.04.2008	38		08.08.2008	54
may			09.08.2008	302
12.05.2008	73		august	
13.05.2008	18		14.08.2008	458
25.05.2008	140		15.08.2008	191
26.05.2008	84		21.08.2008	143
27.05.2008	70		22.08.2008	195
28.05.2008	220		02.09.2008	42
29.05.2008	46		04.09.2008	74
june			05.09.2008	124
01.06.2008	19		08.09.2008	20
04.06.2008	174		09.09.2008	109
05.06.2008	50		10.09.2008	135
06.06.2008	204		september	
07.06.2008	32		20.09.2008	68
10.06.2008	128		21.09.2008	19
11.06.2008	24		28.09.2008	37
13.06.2008	44		29.09.2008	625
17.06.2008	35			
19.06.2008	8			

2. Structural data

Domain St. Ruperti

number	dip direction	dip angle	type
1	182	58	bedding
2	189	60	bedding
3	175	70	bedding
4	165	75	bedding
5	168	72	bedding

6	174	55	bedding
7	173	66	bedding
8	166	56	bedding
9	162	54	bedding
1	326	60	joint
2	324	70	joint
3	306	42	joint
4	280	55	joint
5	288	60	joint
6	284	55	joint
7	258	80	joint
8	256	80	joint
9	250	88	joint
10	104	85	joint
11	88	80	joint
12	105	85	joint
13	236	85	joint
14	240	75	joint
15	248	80	joint
16	324	40	joint
17	322	40	joint
18	326	36	joint
19	350	40	joint
20	350	42	joint
21	336	40	joint
22	92	88	joint
23	81	88	joint
24	85	88	joint
25	282	70	joint
26	284	75	joint
27	280	80	joint
28	285	85	joint
29	282	80	joint
30	91	80	joint
31	109	80	joint
32	85	88	joint
33	94	75	joint
34	96	70	joint
35	80	82	joint
36	92	88	joint
37	85	78	joint
38	314	70	joint
39	328	70	joint
40	318	68	joint
41	78	88	joint
42	70	89	joint
43	82	80	joint
44	240	80	joint
45	254	83	joint
46	244	72	joint

number	dip direction	dip angle	type
1	252	75	slickenside1
2	256	80	slickenside1
3	134	55	lineation1
4	350	50	slickenside2
5	352	50	slickenside2
6	266	20	lineation2
7	322	80	slickenside3
8	332	80	slickenside3
9	242	45	lineation3
10	268	75	slickenside4
11	270	80	slickenside4
12	190	75	lineation4
13	348	65	slickenside5
14	264	10	lineation5
15	334	62	slickenside6
16	243	11	lineation6
17	346	75	slickenside7
18	264	10	lineation7
1	328	10	fault
2	335	30	fault
3	328	23	fault
4	331	20	fault
5	348	30	fault
6	340	15	fault
7	32	65	fault
8	6	55	fault
9	346	60	fault
10	344	52	fault
11	328	85	fault
12	348	75	fault
13	314	80	fault
14	314	85	fault
15	315	88	fault
16	320	50	fault
17	354	20	fault
1	316	55	duplex ramp
2	308	42	duplex flat
3	302	60	duplex ramp
4	304	40	duplex flat
5	342	70	duplex ramp
6	354	50	duplex flat
7	328	58	duplex ramp
8	355	30	duplex flat
9	311	42	duplex flat
10	322	65	duplex ramp
11	328	50	duplex ramp
12	355	40	duplex flat
13	314	35	duplex ramp
14	334	55	duplex flat
15	314	33	duplex flat
16	284	55	duplex ramp
17	352	38	duplex flat

18	318	40	duplex flat
19	262	70	duplex ramp
20	282	40	duplex flat
21	264	80	duplex flat
22	234	45	duplex flat
23	262	75	duplex flat

Domain Oberdoerfl

number	dip direction	dip angle	type
19	178	46	bedding
20	165	45	bedding
21	160	36	bedding
22	164	40	bedding
23	163	53	bedding
24	155	50	bedding
6	242	85	joint
7	300	80	joint
8	276	75	joint
9	296	70	joint
10	290	65	joint
11	286	55	joint
12	301	66	joint
13	13	35	joint
14	14	41	joint
15	30	32	joint
16	44	32	joint
17	55	25	joint
18	25	35	joint
25	56	88	joint
26	44	50	joint
27	76	66	joint
28	81	88	joint
29	64	80	joint
30	46	75	joint
31	240	80	joint
32	241	85	joint
33	268	88	joint
34	280	80	joint
35	220	82	joint
36	246	72	joint

Domain Turiawald

number	dip direction	dip angle	type
1	135	12	bedding
2	216	10	bedding
3	126	16	bedding
4	227	5	bedding

5	141	15	bedding
6	36	6	bedding
7	12	5	bedding
8	304	12	bedding
9	96	4	bedding
10	61	18	bedding
11	311	18	bedding
12	200	16	bedding
13	84	18	bedding
14	103	12	bedding
15	266	9	bedding
16	142	15	bedding
17	134	5	bedding
18	142	12	bedding
19	211	9	bedding
20	212	11	bedding
21	66	11	bedding
22	313	5	bedding
23	69	7	bedding
24	57	16	bedding
25	155	11	bedding
26	1	11	bedding
27	210	11	bedding
28	223	11	bedding
29	346	7	bedding
30	74	5	bedding
31	297	7	bedding
32	38	5	bedding
33	178	11	bedding
34	196	19	bedding
35	225	10	bedding
36	136	15	bedding
37	111	10	bedding
38	115	11	bedding
39	102	10	bedding
40	188	10	bedding
41	34	15	bedding
42	234	10	bedding
43	165	5	bedding
44	48	12	bedding
45	52	10	bedding
46	62	10	bedding
47	75	15	bedding
48	312	4	bedding
49	254	5	bedding
50	104	5	bedding
51	205	3	bedding
52	128	1	bedding
53	210	5	bedding
54	49	3	bedding
55	90	3	bedding
56	324	5	bedding
57	214	10	bedding

58	354	8	bedding
59	336	6	bedding
60	76	3	bedding
61	290	13	bedding
62	336	15	bedding
63	164	10	bedding
64	26	18	bedding
65	0	20	bedding
66	87	20	bedding
67	192	1	bedding
68	314	16	bedding
69	308	15	bedding
70	122	15	bedding
71	102	20	bedding
1	254	23	bedding
2	172	23	bedding
3	123	23	bedding
4	28	25	bedding
5	22	24	bedding
6	312	30	bedding
7	30	40	bedding
8	314	36	bedding
9	352	28	bedding
10	294	30	bedding
1	83	50	joint
2	103	75	joint
3	259	77	joint
4	198	76	joint
5	205	77	joint
6	22	75	joint
7	105	75	joint
8	257	72	joint
9	269	77	joint
10	155	77	joint
11	157	76	joint
12	171	77	joint
13	145	77	joint
14	90	72	joint
15	178	68	joint
16	184	65	joint
17	102	70	joint
18	80	70	joint
19	220	73	joint
20	18	65	joint
21	32	76	joint
22	220	70	joint
23	224	70	joint
24	220	75	joint
1	120	80	joint
2	102	84	joint
3	358	85	joint
4	150	80	joint
5	52	85	joint

6	101	81	joint
7	85	83	joint
8	281	89	joint
9	92	86	joint
10	264	88	joint
11	4	83	joint
12	104	80	joint
13	52	88	joint
14	113	82	joint
15	165	85	joint
16	36	86	joint
17	218	88	joint
18	126	86	joint
19	164	83	joint
20	232	89	joint
21	57	89	joint
22	44	89	joint
23	43	89	joint
24	96	88	joint
25	93	88	joint
26	94	88	joint
27	62	85	joint
28	228	88	joint
29	154	85	joint
30	105	88	joint
31	318	85	joint
32	348	88	joint
33	350	88	joint
34	300	82	joint
35	250	88	joint
36	168	85	joint
37	54	88	joint
38	311	88	joint
39	8	88	joint
40	282	85	joint
41	282	88	joint
42	0	80	joint
43	280	88	joint
44	162	88	joint
45	300	85	joint
46	185	88	joint
47	245	80	joint
48	278	85	joint
49	180	88	joint
50	286	80	joint
51	158	85	joint
52	234	80	joint
53	320	89	joint
54	74	89	joint
55	80	83	joint
56	212	80	joint
57	278	88	joint
58	56	82	joint

59	28	80	joint
60	214	85	joint
61	20	85	joint
62	230	85	joint
63	220	88	joint
64	62	89	joint
65	58	88	joint
66	148	85	joint

Blocks of western slope of Turiawald

number	dip direction	dip angle	type
1	342	33	bedding block
2	96	19	bedding block
3	82	22	bedding block
4	330	30	bedding block
5	352	35	bedding block
6	330	10	bedding block
7	304	18	bedding block
8	275	20	bedding block
9	258	30	bedding block
10	300	22	bedding block
11	104	30	bedding block
12	275	40	bedding block
13	285	30	bedding block
2	351	51	joint block
3	134	75	joint block
4	182	51	joint block
5	89	84	joint block
6	246	81	joint block
7	115	83	joint block
8	244	83	joint block
9	139	40	joint block
10	192	70	joint block
11	159	24	joint block
12	194	75	joint block
13	88	70	joint block

Appendix B

Data of spring logging, as well as mapping results prepared by ArcGis and also the data from appendix A are provided by attached digital data medium.